Accelerated oblique random survival forests

Byron C. Jaeger   BJAEGER@WAKEHEALTH.EDU
Department of Biostatistics and Data Science
Wake Forest University School of Medicine
Winston-Salem, NC 27157, USA

Sawyer Welden   SWELDEN@WAKEHEALTH.EDU
Department of Biostatistics and Data Science
Wake Forest University School of Medicine
Winston-Salem, NC 27157, USA

Kristin Lenoir   KLENOIR@WAKEHEALTH.EDU
Department of Biostatistics and Data Science
Wake Forest University School of Medicine
Winston-Salem, NC 27157, USA

Jaime L Speiser   JSPEISER@WAKEHEALTH.EDU
Department of Biostatistics and Data Science
Wake Forest University School of Medicine
Winston-Salem, NC 27157, USA

Matthew Segar   MATTHEW.SEGAR@UTSOUTHWESTERN.EDU
Division of Cardiology, Department of Internal Medicine,
University of Texas Southwestern Medical Center, Dallas

Nicholas M. Pajewski   NPAJEWSK@WAKEHEALTH.EDU
Department of Biostatistics and Data Science
Wake Forest University School of Medicine
Winston-Salem, NC 27157, USA

Editor: TBD

Abstract

The oblique random survival forest (RSF) is an ensemble supervised learning method for right-censored outcomes. Trees in the oblique RSF are grown using linear combinations of predictors to create branches, whereas in the standard RSF a single predictor is used. Oblique RSF ensembles often have higher prediction accuracy than standard RSF ensembles, but the additional computational overhead of finding an optimal combination of predictors is a severe limitation. In addition, few methods have been developed for interpretation of oblique RSF ensembles. We introduce and evaluate a method to increase computational efficiency of the oblique RSF and a method to estimate importance of individual predictor variables with the oblique RSF. Our strategy to reduce computational overhead makes use of Newton-Raphson scoring, a classical optimization technique that we apply to the Cox partial likelihood function. We estimate importance of predictors for the oblique RSF by negating each coefficient used for the given predictor in linear combinations, and then computing the reduction in out-of-bag accuracy. In numeric experiments, we find that our implementation of the oblique RSF is roughly 500 times faster with equivalent or superior prediction accuracy compared to existing software to fit oblique RSFs. We find in simulation studies that 'negation importance' discriminates between signal and noise predictors more reliably than permutation importance, Shapley additive explanations, and a previously introduced technique to measure variable importance with oblique RSFs based on analysis of variance. All methods pertaining to oblique RSFs in the current study are available in the `aorsf` R package.

Keywords: Random Forests, Survival, Efficient, Variable Importance

1. Introduction

The random survival forest (RSF; Ishwaran et al. (2008); Hothorn et al. (2006)) is a supervised learning algorithm that can be used for risk prediction (Wang and Li, 2017), which may reduce the burden of disease by guiding strategies for prevention and treatment in a wide range of medical domains (Moons et al., 2012a,b). Similar to random forests (RFs) for classification and regression (Breiman, 2001), The RSF is a large set of de-correlated and randomized decision trees, with each tree contributing to the ensemble's prediction function. Notable characteristics of the RSF include uniform convergence of its ensemble survival prediction function to the true survival function, first shown by Ishwaran and Kogalur (2010) and later by Cui et al. (2017) under more general conditions. However, Cui et al. (2017) noted that the RSF is at a disadvantage when predictors are correlated and some are not relevant to the censored outcome, which is a strong possibility when large medical databases are leveraged for risk prediction.

A potential approach to improve the RSF when predictors are correlated and some are not relevant to the censored outcome is to use oblique decision trees instead of axis based trees. Axis based trees split data using a single predictor, creating decision boundaries that are perpendicular or parallel to axes of the predictor space (see Breiman et al., 2017, Chapter 2). Oblique trees split data using a linear combination of predictors, creating decision boundaries that are neither parallel nor perpendicular to axes of their contributing

predictors (see Breiman et al., 2017, Chapter 5). Menze et al. (2011) examined prediction accuracy of RFs in the presence of correlated predictors and found that oblique RFs had substantially higher prediction accuracy compared to axis-based RFs. Similarly, Jaeger et al. (2019) found that growing RSFs with oblique rather than axis-based survival trees reduced the RSF's concordance error, with improvements ranging from 2.5% to 24.9% depending on the data analyzed.

Oblique trees have at least two notable drawbacks compared to axis-based trees. First, finding a locally optimal oblique decision rule may require exponentially more computation than an axis-based rule. If p predictors are potentially used to split n observations, up to $\mathcal{O}(n^p)$ oblique splits can be assessed versus $\mathcal{O}(n \cdot p)$ axis-based splits (Heath et al., 1993; Murthy et al., 1994). Second, estimating variable importance (VI) using permutation (a standard method for RFs) may be less effective in ensembles of oblique trees, as permuting the values of one predictor may not destabilize decisions that are based on many predictors. Although VI is one of the most widely used strategies to interpret random forests (Ishwaran and Lu, 2019), few studies have investigated VI for oblique random forests (see Menze et al., 2011, Section 5), and fewer have investigated VI specifically for the oblique RSF.

This study makes two contributions to oblique RSFs. First, we reduce their computational cost (that is, accelerate them) with a scalable algorithm to identify linear combinations of coefficients. In a general benchmark experiment including 31 risk prediction tasks, we show that accelerated oblique RSFs are roughly 500 times faster with equivalent or superior prediction accuracy compared to existing routines to fit oblique RSFs. Second, we improve their interpretability with 'negation VI', a method to estimate VI that engages with coefficients in linear combinations of predictors instead of permuting predictor values. In simulation studies where VI is estimate using permutation, analysis of variance (ANOVA; see Menze et al. (2011)), and approximations of Shapley values, we find that negation VI improves the oblique RSF's ability to discriminate between correlated signal and noise variables. The accelerated oblique RSF and multiple methods to compute VI for oblique RSFs (permutation, ANOVA, and negation) are available in the `aorsf` R Package.

2. Related work

2.1 Axis-based and oblique random forests

After Breiman (2001) introduced the axis-based and oblique RF, numerous methods were developed to grow oblique RFs for classification or regression tasks (Menze et al., 2011; Zhang and Suganthan, 2014; Rainforth and Wood, 2015; Zhu et al., 2015; Poona et al., 2016; Qiu et al., 2017; Tomita et al., 2020; Katuwal et al., 2020). However, oblique splitting approaches for classification or regression may not generalize to survival (for example, see Zhu, 2013, Section 4.5.1), and most research involving the RSF has focused on forests with axis-based trees (Wang and Li, 2017).

Building on prior research for bagging survival trees (Hothorn et al., 2004), Hothorn et al. (2006) developed an axis-based RSF in their framework for unbiased recursive partitioning, more commonly referred to as the conditional inference forest (CIF). Zhou et al. (2016) developed a rotation forest based on the CIF and Wang and Zhou (2017) developed a method for extending the predictor space of the CIF. Ishwaran et al. (2008) developed an axis-based RSF with strict adherence to the rules for growing trees proposed in Breiman (2001). Jaeger et al. (2019) developed the oblique RSF following the bootstrapping approach described in Breiman's original RF and incorporating early stopping rules from the CIF.

2.2 Variable importance

Breiman (2001) introduced permutation VI, defined for each predictor as the difference in a RF's estimated generalization error before versus after the predictor's values are randomly permuted. Strobl et al. (2007) identified bias in permutation VI driven by variable selection bias and effects induced by bootstrap sampling, and proposed an unbiased permutation VI based on unbiased recursive partitioning (see Hothorn et al. (2006)). Menze et al. (2011) introduced an approach to estimate VI for oblique RFs that computes an analysis of variance (ANOVA) table in non-leaf nodes to obtain p-values for each predictor contributing to the node. The ANOVA VI[1] is then defined for each predictor as the number of times a p-value associated with the predictor is ≤ 0.01 while growing a forest. Lundberg and Lee (2017) introduced a method to estimate VI using SHapley Additive exPlanation (SHAP) values, which estimate the contribution of a predictor to a model's prediction for a given observation. SHAP VI is computed for each predictor by taking the mean absolute value of SHAP values for that predictor across all observations in a given set.

3. The acceleracted oblique random survival forest

Consider the usual framework for survival analysis with training data

$$\mathcal{D}_{\text{train}} = \{(T_i, \delta_i, \boldsymbol{x}_i)\}_{i=1}^{N_{\text{train}}}.$$

Here, T_i is the event time if $\delta_i = 1$ and last point of contact if $\delta_i = 0$, and $\boldsymbol{x}_i$ is a vector of predictors values. Assuming there are no ties, let $t_1 < \ldots < t_m$ denote the m unique event times in $\mathcal{D}_{\text{train}}$.

To accelerate the oblique RSF, we propose to identify linear combinations of predictor variables in non-leaf nodes by applying Newton Raphson scoring to the partial likelihood function of the Cox regression model:

$$L(\boldsymbol{\beta}) = \prod_{i=1}^{m} \frac{e^{\boldsymbol{x}_{j(i)}^T \boldsymbol{\beta}}}{\sum_{j \in R_i} e^{\boldsymbol{x}_j^T \boldsymbol{\beta}}}, \tag{1}$$

---

1. Menze et al. (2011) name their method 'oblique RF VI', but we use the name 'ANOVA VI' in this article to avoid confusing Menze's approach with other approaches to estimate VI for oblique RFs.

where R_i is the set of indices, j, with $T_j \geq t_i$ (i.e., those still at risk at time t_i), and $j(i)$ is the index of the observation for which an event occurred at time t_i. Newton Raphson scoring is an extremely fast estimation procedure, and the `survival` package includes documentation that outlines how to efficiently program it (Therneau, 2022). Briefly, a vector of estimated regression coefficients, $\hat{\beta}$, is updated in each step of the procedure based on its first derivative, $U(\hat{\beta})$, and second derivative, $H(\hat{\beta})$:

$$\hat{\beta}^{k+1} = \hat{\beta}^k + U(\hat{\beta} = \hat{\beta}^k) \, H^{-1}(\hat{\beta} = \hat{\beta}^k)$$

For statistical inference, it is recommended to complete iterations of Newton Raphson scoring until a convergence threshold is met. However, to identify a valid linear combination of predictors, only one iteration of Newton Raphson scoring is needed. In Section 4.1.6, we formally test whether growing oblique survival trees using one iteration of Newton Raphson scoring is sufficient (that is, provides equivalent prediction accuracy) compared to iterating until a convergence threshold is met.

Algorithm 1 presents our approach to fitting an oblique survival tree in the accelerated oblique RSF using default values from the `aorsf` R package. Several steps are taken to reduce computational overhead. First, memory is conserved by conducting bootstrap resampling via randomly generated bootstrap weights. Weights are integer valued, with a weight of v indicating an observation was sampled v times. Second, early stopping is applied to the tree growing procedure if a statistical criterion is not met. In our case, the criterion is based on the magnitude of a log-rank test statistic corresponding to splitting the data at a current node. Third, instead of greedy recursive partitioning, we use a 'good enough' approach. More specifically, instead of computing a log-rank test statistic for several different linear combinations of variables and proceeding with the highest scoring option, we identify an optimal cut-point for one linear combination of variables and assess whether using this combination will create a split that passes the criterion for splitting a node. If it does not pass the criterion, then another linear combination will be tested, with the maximum number of attempts set by the parameter `n_retry`. Often a 'good-enough' split can be found in just one attempt when the training set is large, which gives the accelerated oblique RSF a computational advantage in larger training sets compared to greedy partitioning.

3.1 Negation variable importance

Negation VI is similar to permutation VI in that it measures how much a model's prediction error increases when a variable's role in the model is de-stabilized. More specifically, negation VI measures the increase in an oblique RF's prediction error after flipping the sign of all coefficients linked to a variable (that is, negating them). As the magnitude of a coefficient increases, so does the probability that negating it will change the oblique RF's predictions. For the current study, we use Harrell's concordance (C)-statistic (Harrell et al., 1982) to measure change in prediction error when computing negation VI.

Algorithm 1 Accelerated oblique random survival tree using default parameters.

Require: Training data $\mathcal{D}_{\text{train}} = \{(T_i, \delta_i, \boldsymbol{x}_i)\}_{i=1}^{N_{\text{train}}}$, mtry $= \sqrt{\text{ncol}(\boldsymbol{x}_{\text{train}})}$, n_split $= 5$, n_retry $= 3$, and split_min_stat $= 3.841459$

1: $\mathcal{T} \leftarrow \emptyset$
2: $w \leftarrow \text{sample}(\text{from} = \{0, \dots, 10\}, \text{size} = \text{nrow}(\boldsymbol{x}_{\text{train}}), \text{replace} = \text{T})$
3: $\mathcal{D}_{\text{in-bag}} \leftarrow \text{subset}(\mathcal{D}_{\text{train}}, \text{rows} = \text{which}(w > 0))$
4: $w \leftarrow \text{subset}(w, \text{which}(w > 0))$
5: node_assignments $\leftarrow \text{rep}(1, \text{times} = \text{nrow}(\boldsymbol{x}_{\text{in-bag}}))$
6: nodes_to_split $\leftarrow \{1\}$
7: **repeat**
8:     **for** node $\in$ nodes_to_split **do**
9:         n_try $\leftarrow 1$
10:         node_rows $\leftarrow \text{which}(\text{node\_assignments} \equiv \text{node})$
11:         node_cols $\leftarrow \text{sample}(\text{from} = \{1, \dots, \text{ncol}(\boldsymbol{x})\}, \text{size} = \text{mtry}, \text{replace} = \text{F})$
12:         $\mathcal{D}_{\text{node}} \leftarrow \text{subset}(\mathcal{D}_{\text{in-bag}}, \text{rows} = \text{node\_rows}, \text{columns} = \text{node\_cols})$
13:         $\beta \leftarrow \text{newt\_raph}(\mathcal{D}_{\text{node}}, \text{weights} = \text{subset}(w, \text{node\_rows}), \text{max\_iter} = 1)$
14:         $\eta \leftarrow \boldsymbol{x}_{\text{node}} \times \beta$
15:         $\mathcal{C} \leftarrow \text{sample}(\text{from} = \text{unique}(\eta), \text{size} = \text{n\_split}, \text{replace} = \text{F})$
16:         $c \leftarrow \text{argmax}_{c^* \in \mathcal{C}} \{\text{log\_rank\_stat}(\eta, c^*)\}$
17:         **if** $\text{log\_rank\_stat}(\eta, c) \geq \text{split\_min\_stat}$ **then**
18:             $\mathcal{T} \leftarrow \text{add\_node}(\mathcal{T}, \text{name} = \text{node}, \text{beta} = \beta, \text{cutpoint} = c)$
19:             $\triangleright$ Right node logic omitted for brevity (identical to left node logic)
20:             node_left_name $\leftarrow \text{max}(\text{node\_assignments}) + 1$
21:             node_left_rows $\leftarrow \text{subset}(\text{node\_rows}, \text{which}(\eta \leq c))$
22:             $\text{subset}(\text{node\_assignments}, \text{node\_left\_rows}) \leftarrow \text{node\_left\_name}$
23:             **if** $\text{is\_splittable}(\text{subset}(\text{node\_assignments}, \text{node\_left\_rows}))$ **then**
24:                 nodes_to_split $\leftarrow \text{nodes\_to\_split} \cup \text{node\_left\_name}$
25:             **else**
26:                 $\mathcal{T} \leftarrow \text{add\_leaf}(\mathcal{T}, \text{data} = \text{subset}(\mathcal{D}_{\text{node}}, \text{rows} = \text{node\_left\_rows}))$
27:             **end if**
28:         **else if** n_try $\leq$ n_retry **then**
29:             n_try $\leftarrow$ n_try $+ 1$
30:             **go to** 11
31:         **else**
32:             $\mathcal{T} \leftarrow \text{add\_leaf}(\mathcal{T}, \text{data} = \mathcal{D}_{\text{node}})$
33:         **end if**
34:         nodes_to_split $\leftarrow \text{nodes\_to\_split} \setminus \text{node}$
35:     **end for**
36: **until** nodes_to_split $= \emptyset$
37: **return** $\mathcal{T}$

Negation VI has several characteristics that may be helpful. First, although the current article focuses on oblique RSFs and uses Harrell's C-statistic, negation VI can be applied to any oblique RF using any valid error function.[2]. Second, since the coefficients in each non-leaf node of an oblique tree are adjusted for the accompanying predictors, negation VI may provide better estimation of VI in the presence of correlated variables compared to standard VI techniques. This conjecture is formally assessed in Section 4.2.6. Third, unlike permutation importance, negation VI is non-random and hence reproducible without setting a random seed. Along these lines, since negation VI does not permute variables, the analyst need not worry about impossible combinations of predictors that may occur when one predictor is randomly permuted, such as having a negative status for type 2 diabetes and having Hemoglobin A1c level $\geq 6.5\%$ as a result of randomly permuting the values of Hemoglobin A1c.

4. Numeric experiments

4.1 Benchmark of prediction accuracy and computational efficiency

The aim of this numeric experiment is to evaluate and compare the accelerated oblique RSF with its predecessor (the oblique RSF from the `obliqueRSF` R package) and with other machine learning algorithms for risk prediction. Inferences drawn from this experiment include equivalence and inferiority tests based on Bayesian linear mixed models.

4.1.1 Learners

We consider four classes of learners: RSFs (both axis based and oblique), boosting ensembles, regression models, and neural networks (Table 1). For each class, we synchronized shared tuning parameters. For example, for RSF learners, we set the minimum node size (a parameter shared by all RSF learners) as 10. Additionally, for RSF learners, the number of randomly selected predictors was the square root of the total number of predictors rounded to the nearest integer, and the number of trees in the ensemble was 500. For boosting, regression, and neural network learners, nested 10-fold cross-validation was applied to tune relevant model parameters. Specifically, tuning for boosting models included identifying the number of steps to complete. For regression models, tuning was used to identify the magnitude of penalization. For neural networks, the number and density of layers was tuned.

---

2. The `aorsf` package enables customized functions to be applied in lieu of the default C-statistic (see `?aorsf::orsf_vi_negate`)

Learner Class	Software	Learners	Description
Random Survival Forests			
Axis based	`RandomForestSRC` `ranger` `party` `rotsf` `rsfse`	`rsf-standard` `rsf-extratrees` `cif-standard` `cif-rotate` `cif-spacextend`	`rsf-standard` grows survival trees following Leo Breiman's original random forest algorithm with variables and cut-points selected to maximize a log-rank statistic. `rsf-extratrees` grows survival trees with randomly selected features and cut-points. `cif-standard` uses the framework of conditional inference to grow survival trees. `cif-rotate` extends `cif-standard` by applying principal component analysis to random subsets of data prior to growing each survival tree. `cif-spacextend` derives new predictors for each tree in the ensemble, separately.
Oblique	`obliqueRSF` `aorsf`	`obliqueRSF-net` `aorsf-net` `aorsf-fast` `aorsf-cph` `aorsf-extratrees`	Oblique survival trees following Leo Breiman's random forest algorithm. Linear combinations of inputs are derived using `glmnet` in `obliqueRSF-net` and `aorsf-net`, using Newton Raphson scoring for the Cox partial likelihood function in `aorsf-fast` (1 iteration of scoring) and `aorsf-cph` (up to 20 iterations), and chosen randomly from a uniform distribution in `aorsf-extratrees`. Cut-points are selected from 5 randomly selected candidates to maximize a log-rank statistic.
Boosting ensembles			
Trees	`xgboost`	`xgboost-cox` `xgboost-aft`	`xgboost-cox` maximizes the Cox partial likelihood function, whereas `xgboost-aft` maximizes the accelerated failure time likelihood function. Nested cross validation (5 folds) is applied to tune the number of trees grown, the minimum number of observations in a leaf node was 10, the maximum depth of trees was 6, and $\sqrt{p}$ variables were considered randomly for each tree split, where p is the total number of predictors.
Regression models			
Cox Net	`glmnet`	`glmnet-cox`	The Cox proportional hazards model is fit using an elastic net penalty. Nested cross validation (5 folds) is applied to tune penalty terms.
Neural networks			
Cox Time	`survivalmodels`	`nn-cox`	A neural network based on the proportional hazards model with time-varying effects. Nested cross-validation was applied to select the number of layers (from 1 to 8), the number of nodes in each layer (from $\sqrt{p}/2$ to $\sqrt{p}$), and the number of epochs to complete (up to 500). A drop-out rate of 10% was applied during training.

Table 1: Learning algorithms assessed in numeric studies

4.1.2 EVALUATION OF PREDICTION ACCURACY

Our primary metric for evaluating the accuracy of predicted risk is the integrated and scaled Brier score (Graf et al., 1999). Consider a testing data set:

$$\mathcal{D}_{\text{test}} = \{(T_i, \delta_i, x_i)\}_{i=1}^{N_{\text{test}}}.$$

Let $\widehat{S}(t \mid x_i)$ be the predicted probability of survival up to a given prediction horizon of $t > 0$. For observation i in $\mathcal{D}_{\text{test}}$, let $\widehat{S}(t \mid \boldsymbol{x}_i)$ be the predicted probability of survival up to a given prediction horizon of $t > 0$. Define

$$\widehat{\text{BS}}(t) = \frac{1}{N_{\text{test}}} \sum_{i=1}^{N_{\text{test}}} \{\widehat{S}(t \mid \boldsymbol{x}_i)^2 \cdot I(T_i \leq t, \delta_i = 1) \cdot \widehat{G}(T_i)^{-1}$$
$$+ [1 - \widehat{S}(t \mid \boldsymbol{x}_i)]^2 \cdot I(T_i > t) \cdot \widehat{G}(t)^{-1}\}$$

where $\widehat{G}(t)$ is the Kaplan-Meier estimate of the censoring distribution. As $\widehat{\text{BS}}(t)$ is time dependent, integration over time provides a summary measure of performance over a range of plausible prediction horizons. The integrated $\widehat{\text{BS}}(t)$ is defined as

$$\widehat{\mathcal{BS}}(t_1, t_2) = \frac{1}{t_2 - t_1} \int_{t_1}^{t_2} \widehat{\text{BS}}(t)dt. \tag{2}$$

In our results, t_1 and t_2 are the 25th and 75th percentile of event times, respectively. $\widehat{\mathcal{BS}}(t_1, t_2)$, a sum of squared prediction errors, can be scaled to produce a measure of explained residual variation (that is, an R^2 statistic) by computing

$$R^2 = 1 - \frac{\widehat{\mathcal{BS}}(t_1, t_2)}{\widehat{\mathcal{BS}}_0(t_1, t_2)} \tag{3}$$

where $\widehat{\mathcal{BS}}_0(t_1, t_2)$ is the integrated Brier score when a Kaplan-Meier estimate for survival based on the training data is used as the survival prediction function $\widehat{S}(t)$. We refer to this R^2 statistic as the index of prediction accuracy (IPA) (Kattan and Gerds, 2018).

Our secondary metric for evaluating predicted risk is the time-dependent concordance (C)-statistic. We compute the first time-dependent C-statistic proposed by Blanche et al. (2013, Equation 3), which is interpreted as the probability that a risk prediction model will assign higher risk to a case (that is, an observation with $T \leq t$ and $\delta = 1$) versus a non-case (that is, an observation with $T > t$). Similar to the IPA, observations with $T \leq t$ and $\delta = 0$ only contribute to inverse proportion of censoring weights for the time-dependent C-statistic.

Both the IPA and time-dependent C-statistic generally take values between 0 and 1. To avoid presenting an excessive amount of leading zeroes in our tables, figures, and text, we scale both the IPA and time-dependent C-statistic by 100. For example, we present a value of 25 if the IPA is 0.25, 87 if the time-dependent C-statistic is 0.87, and present 10.2 if the difference between two IPA values is 0.102

4.1.3 DATA SETS

We use a collection of 18 publicly available data sets to benchmark the prediction accuracy and computational efficiency of the accelerated ORSF and each of the other learners described in Section 4.1.1. The number of right-censored outcomes per data set ranged from one to four, and the total number of risk prediction tasks we analyzed was 31 (Table A.1). Across all prediction tasks, the number of observations ranged from 137 to 17,549 (median: 2,231), the number of predictors ranged from 7 to 1,692 (median: 41), and the percentage of censored observations ranged from 5.26 to 97.7 (median: 78.2).

4.1.4 MONTE-CARLO CROSS VALIDATION

For each risk prediction task, we completed 20 runs of Monte-Carlo cross validation. In each run, we used a random sample containing 50% of the available data for training and the remaining 50% for testing each of the learners described in Section 4.1.1. Then, for each learner, we computed the IPA, time-dependent C-statistic, and computational time required to fit a prediction model and compute risk predictions. If any learner failed to obtain predictions on any particular split of data[3], the results for that split were omitted from downstream analyses.

4.1.5 STATISTICAL ANALYSIS

After collecting data from 20 replications of Monte-Carlo cross validation for the 14 learners in all 31 risk prediction tasks, we analyzed the resulting 8,680 observations of IPA and, separately, time-dependent C-statistic, using a Bayesian linear mixed model. Our approach follows the ideas described by Benavoli et al. (2017) and Kuhn and Wickham (2020), who developed guidelines on making statistical comparisons between learners using Bayesian models. Specifically, we fit two models:

$$\text{IPA} = \widehat{\gamma}_0 + \widehat{\gamma} \cdot \text{learner} + (1 \,|\, \text{data/run})$$

and

$$\text{C-stat} = \widehat{\gamma}_0 + \widehat{\gamma} \cdot \text{learner} + (1 \,|\, \text{data/run}).$$

Random intercepts for specific splits of data (that is, `run` in the model formula) were nested within datasets. The intercept, $\widehat{\gamma}_0$, was the expected value of the outcome using `aorsf-fast`, making the coefficients in $\widehat{\gamma}$ the expected differences between `aorsf-fast` and other learners. Default priors from `rstanarm` were applied for model fitting (Goodrich et al., 2022).

---

3. For example, when the prediction task was to predict risk of death in the ACTG 320 clinical trial (26 events total), some splits did not leave enough events in the training data to fit complex learners such as the neural network

Hypothesis testing For both the IPA and time-dependent C-statistic, we conducted equivalence and inferiority tests based on a 1 point region of practical equivalence. More specifically, we concluded that two learners had practically equivalent IPA or time-dependent C-statistic if there was a 95% or higher posterior probability that the absolute difference in the relevant metric was less than 1. We concluded that one learner was weakly superior when there was $\geq 0.95\%$ posterior probability that the difference in the relevant metric was non-zero, and concluded superiority when when there was $\geq 0.95\%$ posterior probability that the difference in the relevant metric was 1 or more.

4.1.6 Results

Index of prediction accuracy Compared to learners that were not oblique RSFs, `aorsf-fast` had the highest IPA in out of 31 risk prediction tasks, with an overall mean IPA of (Figure 1). Compared to the learner with the second highest mean IPA (`rsf-standard`), `aorsf-fast`'s mean was 1.27 points higher, a relative increase of 10.5%. The posterior probability of `aorsf-fast` and `aorsf-cph` having practically equivalent expected IPA was 0.98, and the posterior probability of `aorsf-fast` having a superior IPA to other learners ranged from 0.76 (versus `rsf-standard`) to >0.999 (versus several other learners; see Figure 2)

Time-dependent concordance statistic Compared to learners that were not oblique RSFs, `aorsf-fast` had the highest time-dependent C-statistic in out of 31 risk prediction tasks, with an overall mean of (Figure 3). Compared to the learner with the second highest mean C-statistic (`obliqueRSF-net`), `aorsf-fast`'s mean was 0.643 points higher, a relative increase of 0.837%. The posterior probability of `aorsf-fast` and `aorsf-cph` having practically equivalent expected time-dependent C-statistics was 0.99, and the posterior probability of `aorsf-fast` having a superior time-dependent C-statistic versus other learners ranged from 0.01 (versus `obliqueRSF-net`) to >0.999 (versus several other learners; see Figure 4)

Computational efficiency Overall, `aorsf-fast` was the second fastest learner, with an expected model development and risk prediction time about 1/2 second longer than `glmnet-cox` (Figure 5). Compared to its predecessor, `obliqueRSF-net`, `aorsf-fast` was XYZ times faster.

4.2 Benchmark of variable importance

The aim of this experiment is to evaluate negation VI and similar VI methods based on how well they can discriminate between variables that do or do not have a relationship with a simulated outcome. We consider methods that are intrinsic to the oblique RF (for exampleANOVA VI), those that are intrinsic to the RF (for examplepermutation VI), and those that are model-agnostic (for exampleSHAP VI).

Figure 1: Index of prediction accuracy for the accelerated oblique random survival forest and other learning algorithms across multiple risk prediction tasks. Text appears in tasks where the accelerated oblique random survival forest obtained the highest index of prediction accuracy, showing the absolute and percent improvement over the second best learner.

Learner	Scaled integrated Brier score	Posterior probability		
		Equivalence	Difference < 0	Difference < −1
aorsf−fast		−−−	−−−	−−−
aorsf−cph		0.98	0.60	0.02
aorsf−net		0.65	0.97	0.35
rsf−standard		0.24	>.999	0.76
cif−standard		0.21	>.999	0.79
obliqueRSF−net		0.15	>.999	0.85
cif−rotate		0.15	>.999	0.85
glmnet−cox		0.03	>.999	0.97
ranger−extratrees		0.00	>.999	>.999
cif−extension		0.00	>.999	>.999
aorsf−random		0.00	>.999	>.999
xgboost−cox		0.00	>.999	>.999

Difference versus aorsf−fast
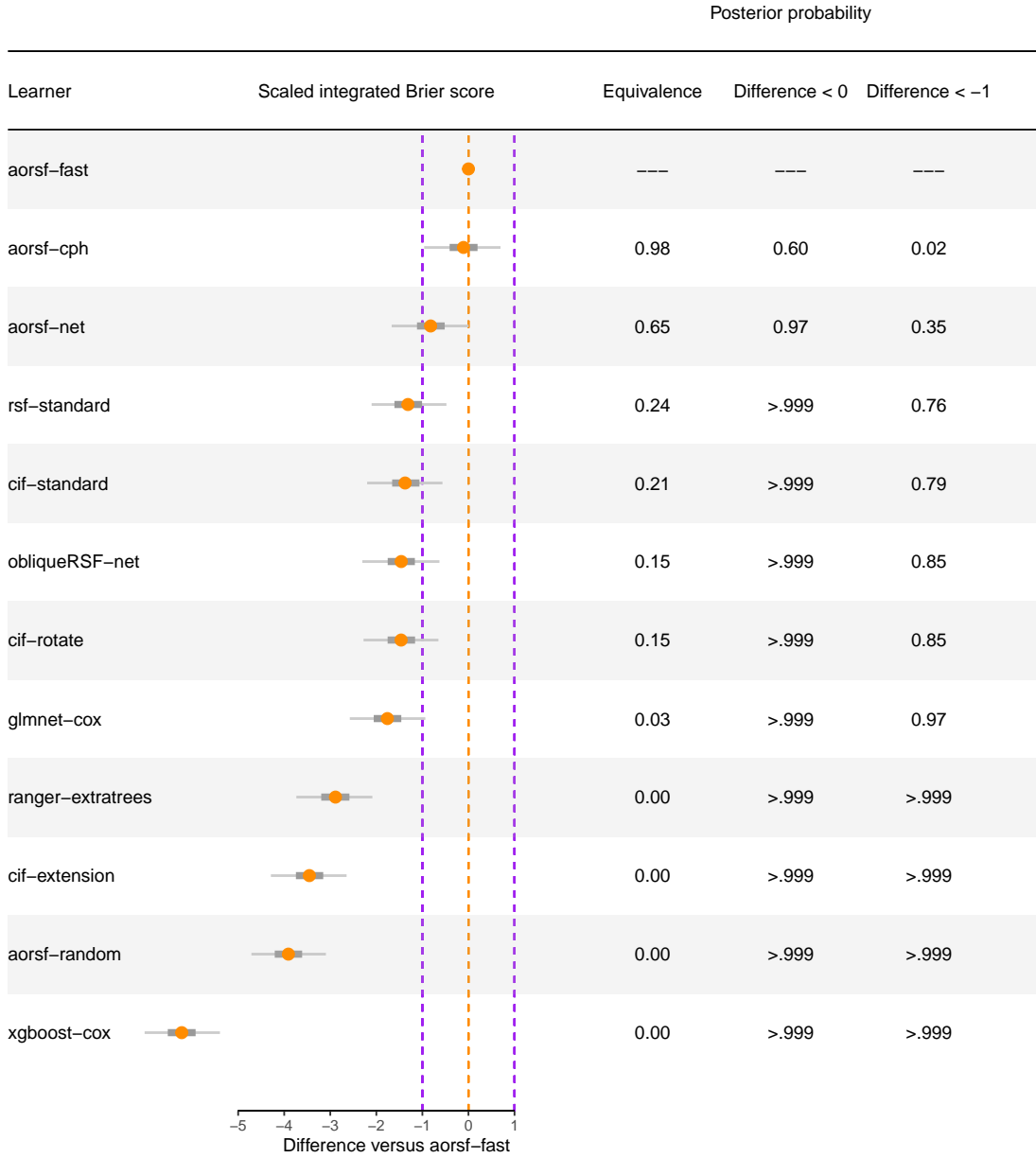
Figure 2: Expected differences in index of prediction accuracy between the accelerated oblique random survival forest and other learning algorithms. A region of practical equivalence is shown by purple dotted lines, and a boundary of non-zero difference is shown by an orange dotted line at the origin.

13
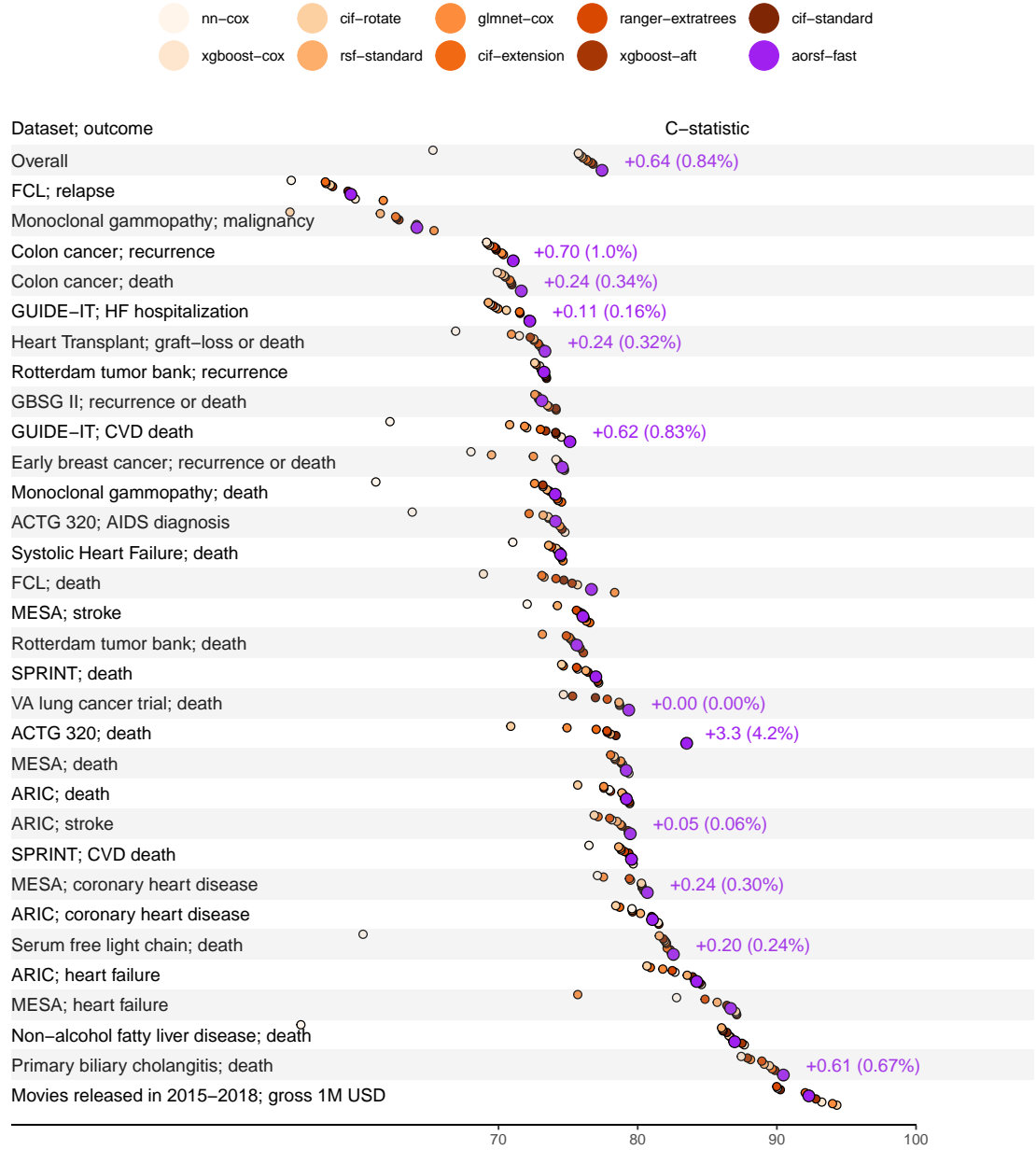
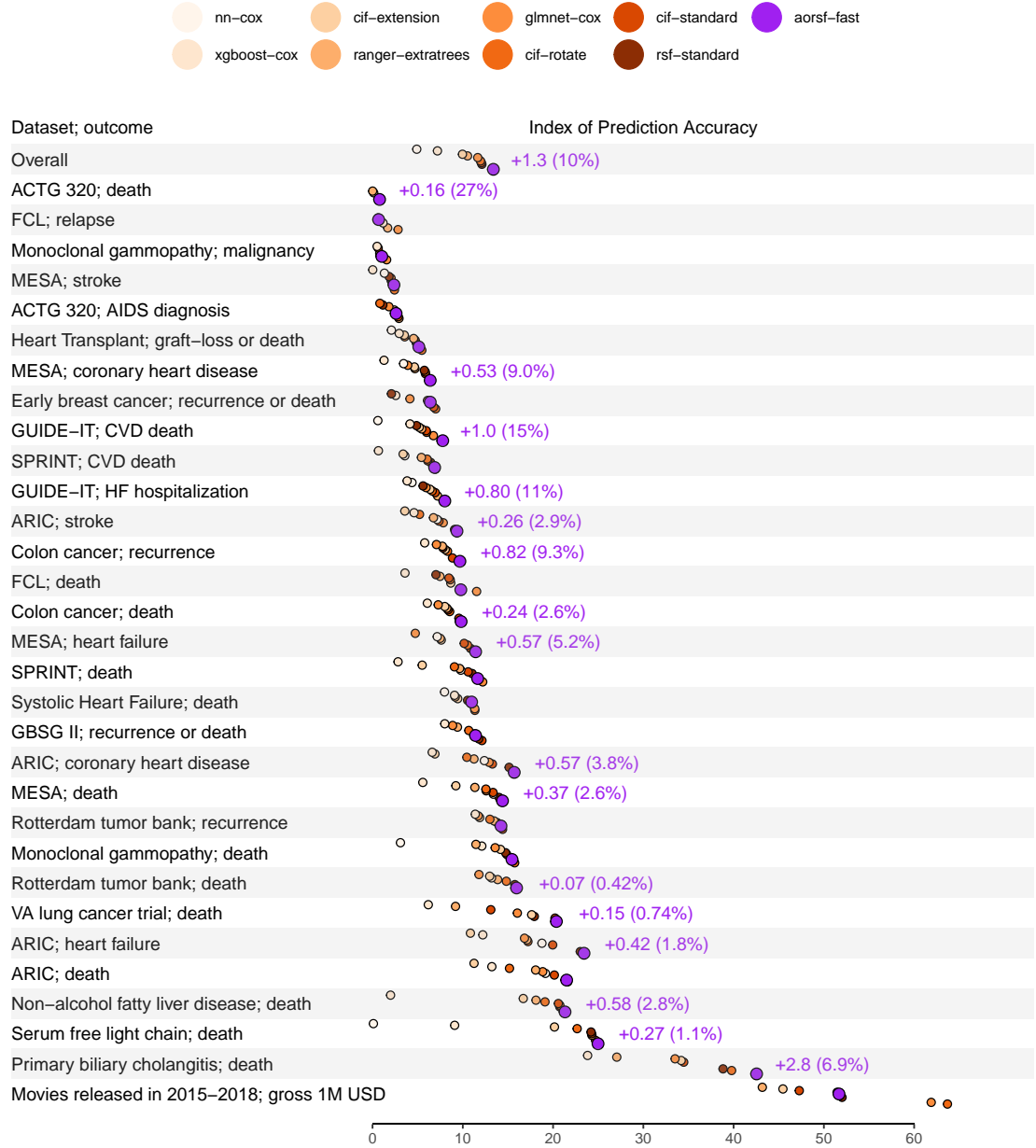Figure 3: Time-dependent concordance statistic for the accelerated oblique random survival forest and other learning algorithms across multiple risk prediction tasks. Text appears in tasks where the accelerated oblique random survival forest obtained the highest concordance, showing the absolute and percent improvement over the second best learner.

		Posterior probability		
Learner	Time−dependent C−statistic	Equivalence	Difference < 0	Difference < −1
aorsf−fast		---	---	---
aorsf−cph		0.99	0.61	0.01
obliqueRSF−net		0.99	0.65	0.01
aorsf−net		0.93	0.90	0.07
cif−standard		0.84	0.96	0.16
ranger−extratrees		0.48	>.999	0.52
cif−extension		0.37	>.999	0.63
glmnet−cox		0.15	>.999	0.85
rsf−standard		0.11	>.999	0.89
cif−rotate		0.04	>.999	0.96
xgboost−cox		0.03	>.999	0.97
aorsf−random		0.00	>.999	>.999

Difference versus aorsf−fast
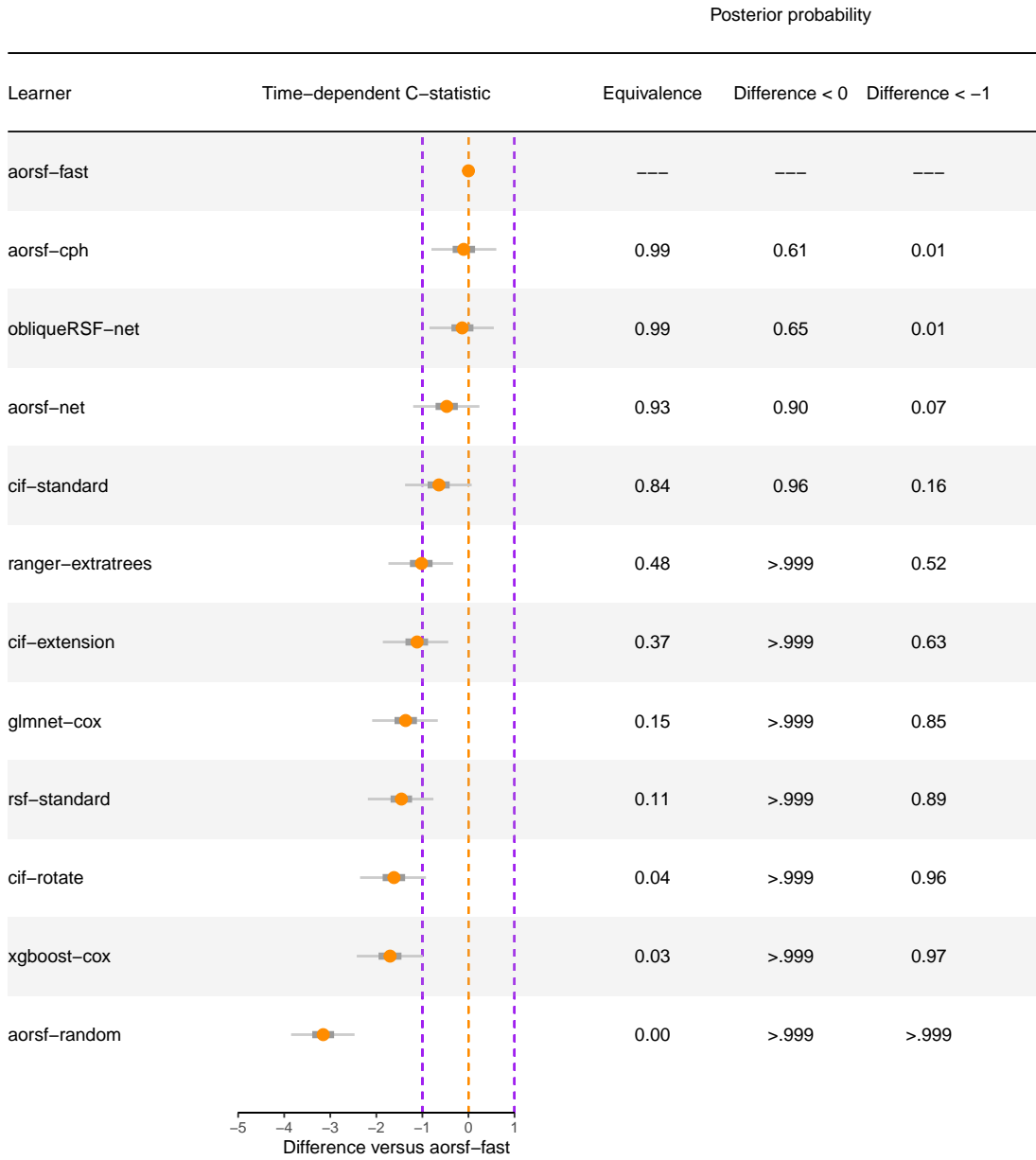
Figure 4: Expected differences in time-dependent concordance statistic between the accelerated oblique random survival forest and other learning algorithms. A region of practical equivalence is shown by purple dotted lines, and a boundary of non-zero difference is shown by an orange dotted line at the origin.

15
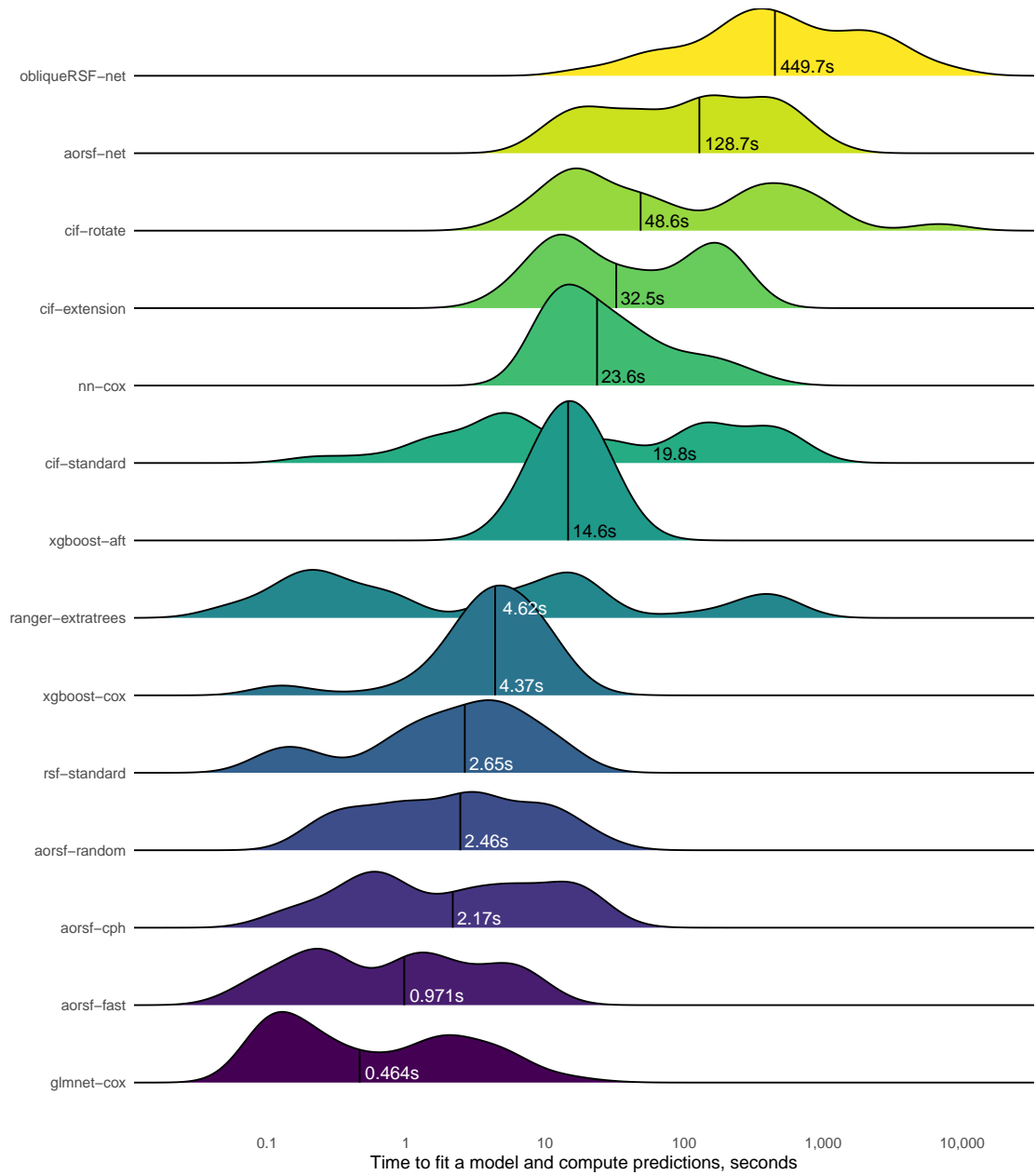
Figure 5: Distribution of time taken to fit a prediction model and compute predicted risk. The median time, in seconds, is printed and annotated for each learner by a vertical line.

4.2.1 Variable importance techniques

We compute permutation VI for axis based RSFs using the `randomForestSRC` package. Although the `party` package implements the approach to VI developed by Strobl et al. (2007), the developers of the `party` package note that the implementation of this approach for survival outcomes is "extremely slow and experimental" as of version 1.3.10. Therefore, it is not incorporated in the current simulation study. We compute ANOVA VI, negation VI, and permutation VI for oblique RSFs using the `aorsf` package. For ANOVA VI, we applied a p-value threshold of 0.01, following the threshold recommended by Menze et al. (2011). We compute SHAP VI for boosted tree models using the `xgboost` package, which incorporates the tree SHAP approach proposed by Lundberg et al. (2018). We also compute SHAP VI for accelerated oblique RSFs using the `fastshap` package.

4.2.2 Variable types

We considered five classes of predictor variables, with each class characterized by its variables' relationship to a right-censored outcome. Specifically,

- *irrelevant* variables had no relationship with the outcome.

- *main effect* variables had a linear relationship to the outcome.

- *non-linear effect* variables had a non-linear relationship to the outcome.

- *combination effect* variables were formed by linear combinations of three other variables. While their combination was linearly related to the outcome, each of the three variables contributing to the combination had no relation to the outcome.

- *interaction effect* variables were related to the outcome by multiplicative interaction with one other variable, which could have been a main effect, non-linear effect, or combination effect variable.

4.2.3 Simulated data

We initiated each set of simulated data with a random draw of size n from a p-dimensional multivariate normal distribution, yielding n observations of p predictors. Each of p predictor variables had a mean of zero, standard deviation of 1, and correlation with other predictor variables drawn at random between a lower and upper boundary. A time-to-event outcome with roughly 45% of observations censored was generated using the `simsurv` package. The full predictor matrix (that is, including interactions, non-linear mappings, and combinations) was used to generate the outcome. Interactions, non-linear mappings, and combinations were dropped from the predictor matrix after the outcome was generated so that VI techniques could be valuated based on their ability to detect these effects.

4.2.4 Parameter specifications

Parameters that varied in the current simulation study included the number of observations (1000, 3000, and 5000) and the minimum and maximum correlation between predictors (-0.1 to 0.1, -0.3 to 0.3, and -0.5 to 0.5). Parameters that remain fixed throughout the study included the number of predictors in each class (15) and the effect size of each predictor, with an increase of one standard deviation associated with a 64% increase in relative risk.

4.2.5 Evaluation of variable importance

We compared VI techniques based on their discrimination (that isC-statistic) between relevant and irrelevant variables. Specifically, we generated a binary outcome for each predictor variable based on its relevance (that is, the binary outcome is 1 if the variable is relevant, 0 otherwise). Treating VI as if it were a 'prediction' for these binary outcomes yields a C-statistic is interpreted as the probability that the VI technique will rank a relevant variable higher than an irrelevant variable (Harrell et al., 1982).

4.2.6 Results

Overall, `aorsf-negate` had the highest C-statistic in 27 out of 36 VI tasks, with an overall mean of 76.1 (Figure 6). Compared to the VI technique with the second highest overall C-statistic (`aorsf-anova`), `aorsf-negate`'s mean was 2.22 points higher, a relative increase of 3.00%. Among the four relevant variable classes, `aorsf-negate` had the highest mean C-statistic for main effects, combination effects, and non-linear effects, with the greatest advantage of using `aorsf-negate` occurring among non-linear and combination variables.

The three techniques that used 'aorsf' to estimate VI were ranked first (negation), second (ANOVA), and third (permutation) in overall mean C-statistic across all of the simulation scenarios. Computationally, ANOVA VI was the fastest technique with a median average

5. Discussion

In this paper, we have developed two contributions to the oblique RSF: (1) the accelerated oblique RSF (that is, `aorsf-fast`) and (2) negation VI. Our technique to accelerate the oblique RSF reduces the number of operations required to find linear combinations of inputs using a single iteration of Newton Raphson scoring, while our VI technique directly engages with coefficients in linear combinations of inputs to measure importance of individual variables. In numeric experiments, we found that that `aorsf-fast` is orders of magnitude more efficient and just as accurate in risk prediction tasks compared to its predecessor, `obliqueRSF-net`. We also found several cases where negation VI allows oblique RSF models to discriminate between relevant and irrelevant variables more effectively than three standard methods to estimate VI: permutation, ANOVA, and SHAP VI. Our results favored negation VI in scenarios where oblique RSFs were the underlying model used to
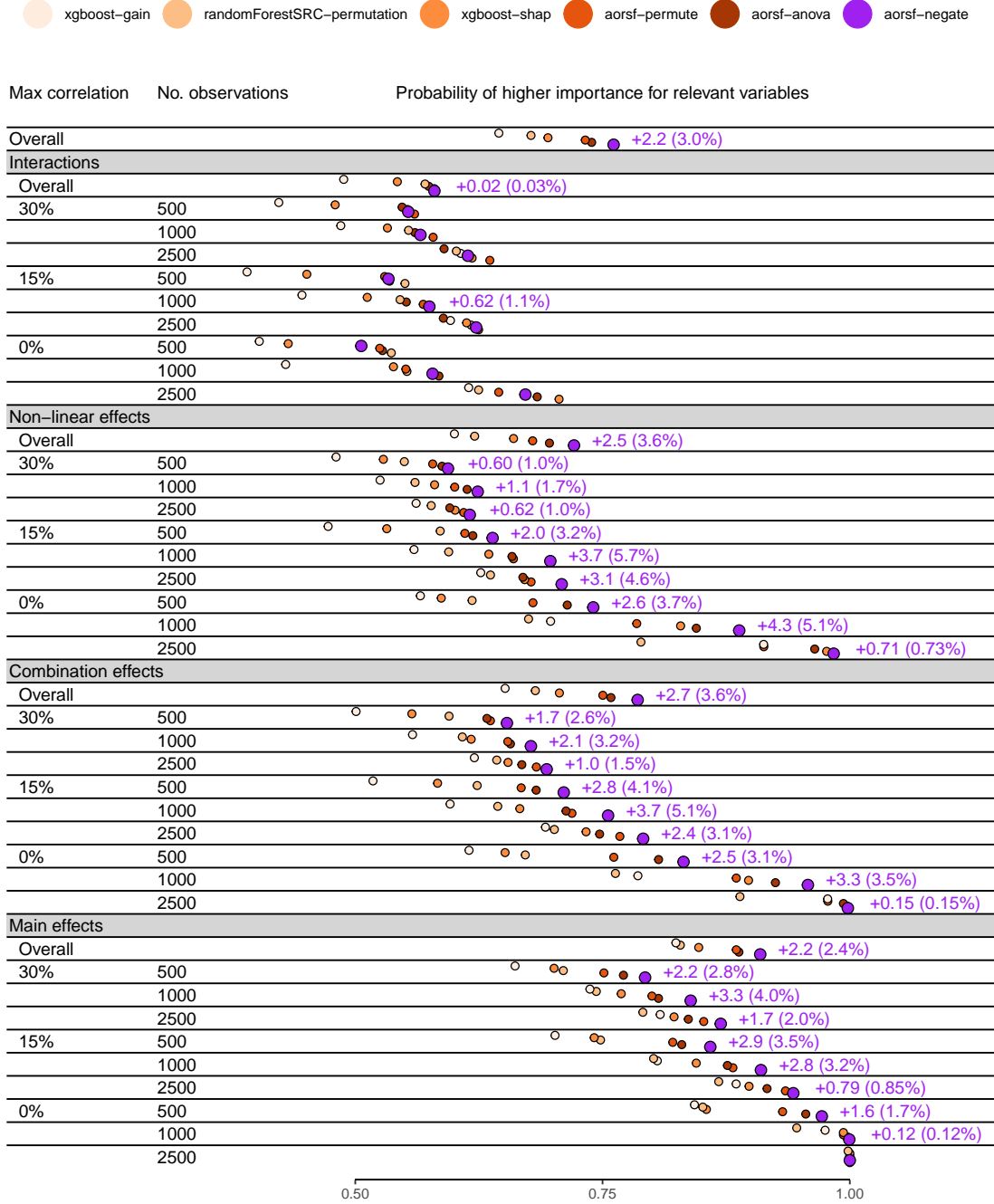
Figure 6: Concordance statistic for assigning higher importance to relevant versus irrelevant variables. Text appears in rows where negation importance obtained the highest concordance, showing absolute and percent improvement over the second best technique.

compute VI and also in scenarios where other modeling techniques (for example, boosted tree ensembles) were used.

5.1 Implications of our results

Accurate risk prediction models have the potential to improve healthcare by directing timely interventions to patients who are most likely to benefit. However, prediction models that cannot be interpreted and explained have no place in clinical practice. The current study advances the oblique RSF, an accurate risk prediction model, towards being accurate, scalable, and interpretable. The improved computational efficiency of the accelerated oblique RSF increases the feasibility of applying oblique RSFs in a wide range of prediction tasks. Faster model evaluation and re-fitting also improve diagnosis and resolution of model-based issues (for example, model calibration deteriorates over time). The introduction of negation VI also advances interpretability. VI is intrinsically linked to model fairness, as it can be used to identify when protected characteristics such as race, religion, and sexuality are inadvertently used (either directly or through correlates of these characteristics) by a prediction model. Since negation VI engages with the coefficients used in linear combinations of variables, a major component of oblique RSFs, it may be more capable of diagnosing unfairness in oblique RSFs compared to permutation importance and model-agnostic VI techniques.

5.2 Limitations and next steps

The current study has several limitations. The accelerated oblique RSF does not account for competing risks, and so our benchmark of prediction accuracy divided tasks where competing risks were present into event-specific tasks. Biased estimation of incidence may occur when competing risks are ignored, and allowing the oblique RSF to account for competing risks is a high priority for future studies. In addition, missing data are not addressed in the accelerated oblique RSF, and users are expected to impute missing values before passing training or testing data into exported functions from the `aorsf` R package. However, missing data are common and it is standard for ensemble tree methods to handle missing data during the tree growing procedure. Thus, a second item of high priority for future studies is to develop and evaluate strategies to handle missing data while growing an oblique RSF. Last, Cui et al. (2017) found that estimating an inverse-probability weighted hazard function at each non-leaf node of a survival tree allows the RSF to converge asymptotically to the true survival function when some variables contribute both to the risk of the event and the risk of censoring, a scenario that is very likely in the analysis of electronic medical records. The accelerated oblique RSF could incorporate this splitting technique by using Newton Raphson scoring to fit a model for the censoring distribution and then a weighted model could be fit to the failure distribution.

Acknowledgments

Appendix

A.1: Data sets used for numeric experiments

Label	N observations	N predictors	Outcome	N Events	% Censored
VA lung cancer trial	137	8	Death	128	6.57
Colon cancer	929	12	Recurrence	468	49.6
			Death	452	51.3
Primary biliary cholangitis	276	19	Death	111	59.8
Movies released in 2015-2018	551	46	Gross 1M USD	522	5.26
GBSG II	686	10	Recurrence Or Death	299	56.4
Systolic Heart Failure	2,231	41	Death	726	67.5
Serum free light chain	7,874	10	Death	2,169	72.5
Non-alcohol fatty liver disease	17,549	24	Death	1,364	92.2
Rotterdam tumor bank	2,982	11	Recurrence	1,518	49.1
			Death	1,272	57.3
ACTG 320	1,151	12	AIDS Diagnosis	96	91.7
			Death	26	97.7
GUIDE-IT	894	59	Cardiovascular Death	110	87.7
			Hf Hospitalization	288	67.8
Early breast cancer	614	1,692	Recurrence Or Death	134	78.2
SPRINT	9,361	174	Cardiovascular Death	521	94.4
			Death	1,644	82.4
Heart Transplant	3,787	52	Graft-Loss Or Death	500	86.8
			Death	76	86.0

FCL	541	7	Relapse	272	49.7
Monoclonal gammopathy	1,384	8	Death	963	30.4
			Malignancy	115	91.7
MESA	6,783	48	Heart Failure	339	95.0
			Coronary Heart Disease	439	93.5
			Stroke	292	95.7
			Death	1,297	80.9
ARIC	13,623	41	Heart Failure	2,981	78.1
			Coronary Heart Disease	2,282	83.2
			Stroke	1,323	90.3
			Death	6,662	51.1

A.2: Index of prediction accuracy, time-dependent concordance statistic, and computational time required to fit and compute predictions for several learning algorithms across 31 risk prediction tasks.

	Performance metric (SD)		Computation time, seconds	
	Scaled Brier	C-Statistic	Model fitting	Risk prediction
Overall				
aorsf-fast	0.134 (0.112)	0.774 (0.071)	0.772	0.188
aorsf-cph	0.133 (0.112)	0.773 (0.070)	1.993	0.184
aorsf-net	0.126 (0.127)	0.770 (0.074)	128.379	0.177
rsf-standard	0.121 (0.116)	0.760 (0.075)	2.168	0.291
cif-standard	0.120 (0.100)	0.768 (0.070)	4.511	15.781
cif-rotate	0.120 (0.128)	0.758 (0.080)	42.206	9.111
obliqueRSF-net	0.120 (0.086)	0.773 (0.071)	376.676	24.742
glmnet-cox	0.117 (0.122)	0.761 (0.075)	0.460	0.004
ranger-extratrees	0.105 (0.088)	0.764 (0.067)	2.416	1.775
cif-extension	0.100 (0.095)	0.763 (0.072)	23.171	8.367
aorsf-random	0.095 (0.083)	0.743 (0.064)	2.272	0.180
xgboost-cox	0.072 (0.102)	0.757 (0.088)	4.368	0.004
nn-cox	0.049 (0.109)	0.653 (0.136)	16.163	4.563
xgboost-aft	-4.74 (5.18)	0.767 (0.074)	14.635	0.007
ACTG 320; AIDS diagnosis, n = 1151, p = 12				
aorsf-random	0.031 (0.020)	0.744 (0.035)	0.408	0.036
ranger-extratrees	0.029 (0.017)	0.739 (0.037)	0.052	0.145
cif-standard	0.028 (0.027)	0.746 (0.039)	1.052	4.532
obliqueRSF-net	0.028 (0.022)	0.743 (0.039)	26.784	15.942
aorsf-fast	0.026 (0.027)	0.741 (0.041)	0.143	0.034
aorsf-cph	0.026 (0.029)	0.747 (0.040)	0.433	0.035
cif-extension	0.024 (0.015)	0.722 (0.040)	9.266	4.180
aorsf-net	0.020 (0.034)	0.742 (0.040)	18.859	0.036
glmnet-cox	0.018 (0.027)	0.744 (0.035)	0.172	0.002
rsf-standard	0.011 (0.034)	0.732 (0.042)	0.145	0.059
cif-rotate	0.008 (0.037)	0.736 (0.035)	15.338	3.967
nn-cox	-0.001 (0.017)	0.638 (0.114)	10.944	0.541
xgboost-cox	-0.002 (0.048)	0.748 (0.033)	3.788	0.003
xgboost-aft	-8.09 (1.44)	0.736 (0.035)	9.657	0.006
ACTG 320; death, n = 1151, p = 12				
aorsf-fast	0.008 (0.019)	0.835 (0.056)	0.087	0.020
obliqueRSF-net	0.008 (0.011)	0.829 (0.053)	8.678	10.534

A.2: Index of prediction accuracy, time-dependent concordance statistic, and computational time required to fit and compute predictions for several learning algorithms across 31 risk prediction tasks. *(continued)*

	Scaled Brier	C-Statistic	Model fitting	Risk prediction
aorsf-cph	0.008 (0.018)	0.827 (0.063)	0.351	0.020
aorsf-random	0.006 (0.014)	0.802 (0.071)	0.224	0.023
cif-extension	0.001 (0.021)	0.770 (0.069)	8.850	3.780
ranger-extratrees	0.000 (0.019)	0.778 (0.073)	0.041	0.126
aorsf-net	-0.002 (0.032)	0.814 (0.069)	14.142	0.023
cif-standard	-0.004 (0.025)	0.784 (0.065)	1.106	4.570
xgboost-cox	-0.004 (0.004)	0.500 (0.000)	0.111	0.002
nn-cox	-0.005 (0.004)	0.522 (0.099)	9.961	0.534
rsf-standard	-0.028 (0.050)	0.780 (0.078)	0.093	0.037
cif-rotate	-0.036 (0.048)	0.709 (0.091)	13.345	3.439
glmnet-cox	-0.060 (0.102)	0.749 (0.106)	0.275	0.002
xgboost-aft	-25.1 (7.60)	0.778 (0.074)	9.772	0.006
ARIC; coronary heart disease, n = 13623, p = 41				
aorsf-fast	0.157 (0.007)	0.811 (0.007)	4.591	1.355
aorsf-cph	0.153 (0.007)	0.810 (0.007)	14.698	1.385
aorsf-net	0.153 (0.007)	0.811 (0.007)	507.224	1.477
rsf-standard	0.151 (0.007)	0.802 (0.007)	9.099	1.101
obliqueRSF-net	0.144 (0.005)	0.813 (0.007)	2836.384	351.006
cif-standard	0.133 (0.005)	0.810 (0.007)	70.288	358.500
glmnet-cox	0.129 (0.012)	0.796 (0.008)	1.721	0.011
nn-cox	0.124 (0.014)	0.796 (0.007)	55.992	105.741
ranger-extratrees	0.112 (0.005)	0.796 (0.008)	320.882	71.239
cif-rotate	0.104 (0.004)	0.784 (0.008)	569.756	70.690
aorsf-random	0.098 (0.005)	0.773 (0.008)	11.738	1.361
cif-extension	0.069 (0.002)	0.787 (0.009)	164.896	51.659
xgboost-cox	0.066 (0.018)	0.815 (0.006)	8.635	0.015
xgboost-aft	-4.92 (0.295)	0.815 (0.005)	22.322	0.013
ARIC; death, n = 13623, p = 41				
aorsf-net	0.217 (0.006)	0.792 (0.004)	952.688	2.390
rsf-standard	0.216 (0.007)	0.789 (0.004)	13.694	1.330
aorsf-fast	0.215 (0.007)	0.792 (0.004)	7.760	2.287
aorsf-cph	0.215 (0.007)	0.791 (0.004)	23.194	2.305
obliqueRSF-net	0.207 (0.005)	0.791 (0.004)	7578.159	316.772
cif-standard	0.201 (0.005)	0.790 (0.004)	72.192	385.603
nn-cox	0.192 (0.013)	0.780 (0.005)	102.206	101.400

A.2: Index of prediction accuracy, time-dependent concordance statistic, and computational time required to fit and compute predictions for several learning algorithms across 31 risk prediction tasks. *(continued)*

	Scaled Brier	C-Statistic	Model fitting	Risk prediction
glmnet-cox	0.189 (0.015)	0.776 (0.007)	2.123	0.012
ranger-extratrees	0.181 (0.005)	0.781 (0.005)	421.367	67.011
cif-rotate	0.152 (0.007)	0.757 (0.006)	582.264	65.718
xgboost-cox	0.132 (0.011)	0.794 (0.004)	12.326	0.016
aorsf-random	0.130 (0.005)	0.733 (0.006)	22.918	2.061
cif-extension	0.112 (0.002)	0.776 (0.005)	182.973	54.549
xgboost-aft	-1.59 (0.150)	0.794 (0.004)	28.205	0.015
ARIC; heart failure, n = 13623, p = 41				
aorsf-fast	0.234 (0.007)	0.842 (0.005)	5.447	1.627
rsf-standard	0.230 (0.007)	0.836 (0.005)	10.044	1.063
aorsf-cph	0.230 (0.006)	0.841 (0.005)	16.965	1.635
aorsf-net	0.216 (0.059)	0.832 (0.045)	632.139	1.707
obliqueRSF-net	0.213 (0.005)	0.842 (0.005)	3706.701	311.291
cif-standard	0.200 (0.004)	0.839 (0.005)	74.710	369.280
nn-cox	0.188 (0.020)	0.827 (0.009)	66.425	104.654
cif-rotate	0.172 (0.006)	0.807 (0.007)	577.084	67.496
ranger-extratrees	0.171 (0.004)	0.825 (0.005)	326.124	84.602
glmnet-cox	0.168 (0.042)	0.818 (0.016)	2.513	0.012
aorsf-random	0.139 (0.005)	0.789 (0.006)	15.868	1.587
xgboost-cox	0.122 (0.017)	0.846 (0.005)	11.223	0.015
cif-extension	0.108 (0.003)	0.809 (0.007)	169.585	49.274
xgboost-aft	-3.80 (0.250)	0.845 (0.005)	26.160	0.014
ARIC; stroke, n = 13623, p = 41				
aorsf-fast	0.094 (0.004)	0.795 (0.007)	4.109	1.124
rsf-standard	0.091 (0.005)	0.785 (0.007)	7.142	0.915
aorsf-cph	0.090 (0.004)	0.793 (0.008)	13.304	1.124
aorsf-net	0.087 (0.018)	0.786 (0.032)	391.565	1.201
obliqueRSF-net	0.082 (0.003)	0.792 (0.007)	1773.436	379.126
glmnet-cox	0.078 (0.005)	0.788 (0.007)	1.789	0.010
cif-standard	0.074 (0.003)	0.789 (0.007)	72.507	366.228
nn-cox	0.072 (0.013)	0.781 (0.010)	32.716	93.157
ranger-extratrees	0.068 (0.003)	0.780 (0.009)	256.826	67.732
aorsf-random	0.059 (0.004)	0.751 (0.009)	9.314	1.118
cif-rotate	0.052 (0.003)	0.769 (0.009)	588.245	70.061
xgboost-cox	0.046 (0.014)	0.794 (0.006)	6.688	0.014

A.2: Index of prediction accuracy, time-dependent concordance statistic, and computational time required to fit and compute predictions for several learning algorithms across 31 risk prediction tasks. *(continued)*

	Scaled Brier	C-Statistic	Model fitting	Risk prediction
cif-extension	0.036 (0.002)	0.772 (0.008)	169.525	51.117
xgboost-aft	-6.54 (0.420)	0.793 (0.007)	21.053	0.013
Colon cancer; death, n = 929, p = 12				
aorsf-fast	0.098 (0.014)	0.716 (0.012)	0.228	0.050
aorsf-cph	0.098 (0.014)	0.715 (0.011)	0.632	0.051
cif-standard	0.096 (0.014)	0.709 (0.012)	0.666	3.606
aorsf-random	0.094 (0.009)	0.714 (0.011)	1.002	0.045
aorsf-net	0.090 (0.025)	0.708 (0.037)	49.445	0.046
obliqueRSF-net	0.088 (0.006)	0.716 (0.012)	250.492	16.952
cif-rotate	0.085 (0.018)	0.704 (0.014)	12.226	3.491
rsf-standard	0.084 (0.019)	0.702 (0.010)	1.526	0.149
ranger-extratrees	0.082 (0.007)	0.710 (0.011)	0.090	0.245
cif-extension	0.080 (0.006)	0.708 (0.012)	8.368	4.020
glmnet-cox	0.073 (0.014)	0.709 (0.017)	0.104	0.003
xgboost-cox	0.061 (0.013)	0.699 (0.012)	3.172	0.003
nn-cox	-0.003 (0.003)	0.511 (0.022)	11.966	1.368
xgboost-aft	-1.12 (0.214)	0.705 (0.014)	11.661	0.006
Colon cancer; recurrence, n = 929, p = 12				
aorsf-fast	0.097 (0.016)	0.711 (0.015)	0.228	0.050
aorsf-cph	0.096 (0.017)	0.710 (0.014)	0.641	0.050
cif-standard	0.089 (0.016)	0.698 (0.015)	0.661	3.398
obliqueRSF-net	0.086 (0.009)	0.708 (0.014)	258.163	16.636
aorsf-net	0.085 (0.044)	0.705 (0.025)	50.808	0.048
aorsf-random	0.085 (0.013)	0.700 (0.015)	0.998	0.047
cif-rotate	0.083 (0.020)	0.694 (0.016)	12.335	3.554
cif-extension	0.081 (0.008)	0.704 (0.015)	8.129	3.884
rsf-standard	0.078 (0.021)	0.692 (0.014)	1.621	0.147
ranger-extratrees	0.077 (0.011)	0.697 (0.014)	0.090	0.238
glmnet-cox	0.071 (0.018)	0.702 (0.024)	0.115	0.003
xgboost-cox	0.058 (0.010)	0.691 (0.016)	3.002	0.003
nn-cox	-0.014 (0.033)	0.502 (0.035)	13.490	1.248
xgboost-aft	-1.22 (0.257)	0.698 (0.017)	12.295	0.006
Early breast cancer; recurrence or death, n = 614, p = 1692				
obliqueRSF-net	0.072 (0.024)	0.750 (0.028)	1858.856	13.453

A.2: Index of prediction accuracy, time-dependent concordance statistic, and computational time required to fit and compute predictions for several learning algorithms across 31 risk prediction tasks. *(continued)*

	Scaled Brier	C-Statistic	Model fitting	Risk prediction
cif-rotate	0.070 (0.018)	0.747 (0.028)	6486.756	347.401
cif-standard	0.068 (0.018)	0.747 (0.028)	8.224	4.008
aorsf-cph	0.065 (0.031)	0.744 (0.023)	1.313	0.182
cif-extension	0.065 (0.015)	0.746 (0.026)	43.993	6.218
aorsf-fast	0.064 (0.030)	0.746 (0.024)	0.746	0.180
ranger-extratrees	0.061 (0.023)	0.743 (0.028)	0.218	0.658
glmnet-cox	0.041 (0.032)	0.725 (0.035)	5.758	0.006
aorsf-random	0.027 (0.015)	0.693 (0.039)	1.671	0.174
xgboost-cox	0.026 (0.035)	0.741 (0.028)	2.272	0.007
rsf-standard	0.021 (0.041)	0.695 (0.032)	0.777	0.314
nn-cox	-0.020 (0.076)	0.680 (0.050)	16.928	1.662
aorsf-net	-0.048 (0.260)	0.730 (0.055)	455.331	0.176
xgboost-aft	-3.08 (0.662)	0.742 (0.024)	9.532	0.010
FCL; death, n = 541, p = 7				
glmnet-cox	0.115 (0.031)	0.783 (0.037)	0.091	0.002
aorsf-fast	0.098 (0.040)	0.767 (0.032)	0.079	0.019
aorsf-cph	0.097 (0.041)	0.768 (0.033)	0.166	0.019
aorsf-net	0.092 (0.043)	0.750 (0.051)	13.196	0.019
obliqueRSF-net	0.090 (0.029)	0.760 (0.038)	96.051	5.285
cif-extension	0.087 (0.039)	0.731 (0.038)	5.172	2.488
aorsf-random	0.086 (0.030)	0.757 (0.034)	0.267	0.019
cif-rotate	0.086 (0.053)	0.757 (0.030)	6.010	2.042
cif-standard	0.085 (0.040)	0.747 (0.036)	0.290	1.114
ranger-extratrees	0.075 (0.016)	0.741 (0.033)	0.044	0.083
rsf-standard	0.070 (0.052)	0.733 (0.037)	0.109	0.038
xgboost-cox	0.036 (0.054)	0.689 (0.112)	0.348	0.002
nn-cox	-0.003 (0.023)	0.527 (0.112)	11.211	0.423
xgboost-aft	-2.56 (0.515)	0.753 (0.039)	7.831	0.006
FCL; relapse, n = 541, p = 7				
glmnet-cox	0.028 (0.018)	0.617 (0.024)	0.089	0.002
ranger-extratrees	0.017 (0.016)	0.593 (0.026)	0.033	0.081
obliqueRSF-net	0.013 (0.016)	0.590 (0.025)	217.653	6.187
aorsf-random	0.012 (0.018)	0.595 (0.026)	0.395	0.021
xgboost-cox	0.012 (0.015)	0.597 (0.032)	1.357	0.002
aorsf-cph	0.007 (0.022)	0.595 (0.027)	0.262	0.023

29

A.2: Index of prediction accuracy, time-dependent concordance statistic, and computational time required to fit and compute predictions for several learning algorithms across 31 risk prediction tasks. *(continued)*

	Scaled Brier	C-Statistic	Model fitting	Risk prediction
aorsf-fast	0.007 (0.021)	0.594 (0.026)	0.111	0.022
cif-standard	0.006 (0.020)	0.592 (0.023)	0.293	1.114
aorsf-net	0.006 (0.022)	0.591 (0.028)	19.287	0.022
nn-cox	-0.001 (0.023)	0.551 (0.062)	11.433	0.439
cif-extension	-0.007 (0.024)	0.576 (0.029)	5.918	2.338
cif-rotate	-0.016 (0.026)	0.579 (0.031)	7.022	1.987
rsf-standard	-0.028 (0.033)	0.576 (0.026)	0.833	0.086
xgboost-aft	-0.897 (0.328)	0.581 (0.037)	6.337	0.006
GBSG II; recurrence or death, n = 686, p = 10				
obliqueRSF-net	0.122 (0.015)	0.744 (0.017)	313.230	6.842
cif-standard	0.121 (0.020)	0.741 (0.020)	0.426	1.769
rsf-standard	0.118 (0.024)	0.735 (0.020)	1.394	0.116
aorsf-cph	0.117 (0.026)	0.734 (0.018)	0.407	0.038
aorsf-fast	0.114 (0.025)	0.731 (0.017)	0.171	0.039
cif-extension	0.113 (0.018)	0.741 (0.020)	8.106	3.385
aorsf-net	0.109 (0.058)	0.732 (0.036)	37.488	0.038
cif-rotate	0.107 (0.025)	0.729 (0.018)	10.819	2.645
aorsf-random	0.103 (0.025)	0.722 (0.026)	0.786	0.036
ranger-extratrees	0.094 (0.019)	0.736 (0.025)	0.051	0.136
glmnet-cox	0.089 (0.018)	0.726 (0.021)	0.098	0.002
xgboost-cox	0.080 (0.017)	0.729 (0.018)	2.465	0.003
nn-cox	-0.003 (0.005)	0.524 (0.052)	11.570	0.838
xgboost-aft	-1.10 (0.165)	0.728 (0.022)	10.557	0.006
GUIDE-IT; CVD death, n = 894, p = 59				
aorsf-fast	0.078 (0.017)	0.751 (0.026)	0.160	0.037
aorsf-net	0.076 (0.017)	0.748 (0.027)	27.393	0.039
aorsf-cph	0.073 (0.019)	0.746 (0.029)	0.379	0.037
glmnet-cox	0.067 (0.042)	0.719 (0.087)	0.498	0.003
obliqueRSF-net	0.064 (0.013)	0.744 (0.023)	221.509	11.260
cif-rotate	0.060 (0.014)	0.720 (0.025)	34.884	5.270
cif-standard	0.059 (0.014)	0.741 (0.023)	0.880	3.606
ranger-extratrees	0.054 (0.013)	0.741 (0.030)	0.091	0.178
cif-extension	0.052 (0.012)	0.730 (0.024)	13.387	5.416
rsf-standard	0.049 (0.022)	0.708 (0.027)	0.169	0.058
xgboost-cox	0.041 (0.045)	0.745 (0.018)	3.691	0.003

A.2: Index of prediction accuracy, time-dependent concordance statistic, and computational time required to fit and compute predictions for several learning algorithms across 31 risk prediction tasks. *(continued)*

	Scaled Brier	C-Statistic	Model fitting	Risk prediction
aorsf-random	0.033 (0.013)	0.700 (0.029)	0.499	0.039
nn-cox	0.006 (0.017)	0.622 (0.088)	10.440	0.558
xgboost-aft	-5.08 (1.03)	0.734 (0.021)	10.919	0.006
GUIDE-IT; HF hospitalization, n = 894, p = 59				
aorsf-fast	0.080 (0.020)	0.722 (0.027)	0.241	0.053
aorsf-cph	0.080 (0.019)	0.721 (0.025)	0.691	0.054
obliqueRSF-net	0.073 (0.011)	0.720 (0.025)	382.054	9.235
ranger-extratrees	0.072 (0.010)	0.721 (0.023)	0.107	0.191
aorsf-net	0.072 (0.043)	0.716 (0.037)	53.293	0.057
cif-standard	0.069 (0.011)	0.715 (0.025)	0.802	3.237
cif-rotate	0.066 (0.020)	0.706 (0.031)	41.812	5.179
cif-extension	0.064 (0.009)	0.715 (0.023)	14.460	5.513
glmnet-cox	0.059 (0.021)	0.700 (0.026)	0.453	0.003
rsf-standard	0.056 (0.023)	0.693 (0.027)	1.503	0.119
aorsf-random	0.049 (0.010)	0.683 (0.024)	0.914	0.053
nn-cox	0.044 (0.027)	0.694 (0.041)	12.746	0.589
xgboost-cox	0.038 (0.018)	0.698 (0.028)	2.920	0.003
xgboost-aft	-2.24 (0.328)	0.696 (0.027)	13.125	0.006
Heart Transplant; graft-loss or death, n = 3787, p = 52				
cif-rotate	0.055 (0.010)	0.729 (0.017)	158.010	21.041
aorsf-net	0.052 (0.006)	0.730 (0.013)	126.426	0.231
aorsf-fast	0.051 (0.007)	0.733 (0.015)	0.875	0.222
aorsf-cph	0.051 (0.006)	0.732 (0.014)	3.009	0.226
cif-standard	0.049 (0.007)	0.731 (0.014)	10.227	36.786
obliqueRSF-net	0.048 (0.006)	0.728 (0.015)	365.007	70.588
rsf-standard	0.047 (0.010)	0.725 (0.013)	2.462	0.933
ranger-extratrees	0.046 (0.007)	0.729 (0.014)	5.510	3.387
glmnet-cox	0.036 (0.006)	0.709 (0.016)	0.969	0.005
cif-extension	0.035 (0.004)	0.725 (0.018)	49.685	18.172
xgboost-cox	0.030 (0.007)	0.715 (0.019)	3.479	0.005
aorsf-random	0.028 (0.003)	0.689 (0.013)	2.461	0.218
nn-cox	0.021 (0.013)	0.669 (0.043)	15.828	9.990
xgboost-aft	-4.46 (0.518)	0.723 (0.013)	14.471	0.007
MESA; coronary heart disease, n = 6785, p = 48				

A.2: Index of prediction accuracy, time-dependent concordance statistic, and computational time required to fit and compute predictions for several learning algorithms across 31 risk prediction tasks. *(continued)*

	Scaled Brier	C-Statistic	Model fitting	Risk prediction
aorsf-fast	0.064 (0.010)	0.807 (0.010)	1.254	0.359
aorsf-net	0.063 (0.010)	0.804 (0.010)	174.770	0.380
obliqueRSF-net	0.062 (0.008)	0.809 (0.009)	489.721	264.595
aorsf-cph	0.061 (0.010)	0.801 (0.012)	5.084	0.365
cif-standard	0.059 (0.006)	0.803 (0.011)	23.030	98.735
cif-rotate	0.058 (0.007)	0.803 (0.010)	290.894	38.516
rsf-standard	0.057 (0.012)	0.795 (0.012)	3.507	1.082
ranger-extratrees	0.047 (0.004)	0.794 (0.010)	7.733	6.984
cif-extension	0.046 (0.003)	0.805 (0.010)	99.785	30.035
glmnet-cox	0.039 (0.017)	0.775 (0.016)	4.983	0.007
nn-cox	0.034 (0.014)	0.771 (0.018)	16.832	16.923
aorsf-random	0.031 (0.005)	0.735 (0.015)	3.622	0.410
xgboost-cox	0.013 (0.020)	0.803 (0.010)	4.416	0.008
xgboost-aft	-9.73 (1.00)	0.803 (0.010)	19.012	0.009
MESA; death, n = 6793, p = 48				
aorsf-net	0.144 (0.008)	0.791 (0.009)	302.684	0.545
aorsf-fast	0.144 (0.008)	0.792 (0.010)	1.785	0.630
aorsf-cph	0.143 (0.007)	0.791 (0.009)	6.757	0.532
rsf-standard	0.140 (0.008)	0.783 (0.009)	4.567	0.475
obliqueRSF-net	0.139 (0.007)	0.791 (0.010)	1155.438	154.187
nn-cox	0.134 (0.012)	0.789 (0.010)	32.143	19.831
cif-standard	0.133 (0.006)	0.788 (0.009)	23.210	99.971
glmnet-cox	0.126 (0.026)	0.788 (0.012)	1.504	0.006
cif-rotate	0.126 (0.007)	0.783 (0.010)	318.556	36.862
ranger-extratrees	0.113 (0.004)	0.784 (0.009)	7.675	6.070
cif-extension	0.092 (0.003)	0.781 (0.009)	110.511	30.598
aorsf-random	0.069 (0.005)	0.725 (0.008)	5.706	0.551
xgboost-cox	0.056 (0.030)	0.794 (0.010)	8.559	0.010
xgboost-aft	-4.42 (0.238)	0.792 (0.009)	22.063	0.009
MESA; heart failure, n = 6785, p = 48				
aorsf-fast	0.114 (0.011)	0.867 (0.012)	1.145	0.317
aorsf-cph	0.109 (0.012)	0.859 (0.014)	4.847	0.330
rsf-standard	0.109 (0.012)	0.857 (0.011)	3.064	1.083
obliqueRSF-net	0.106 (0.008)	0.869 (0.012)	402.559	332.725
cif-rotate	0.105 (0.010)	0.870 (0.012)	262.282	37.634

A.2: Index of prediction accuracy, time-dependent concordance statistic, and computational time required to fit and compute predictions for several learning algorithms across 31 risk prediction tasks. *(continued)*

	Scaled Brier	C-Statistic	Model fitting	Risk prediction
cif-standard	0.101 (0.009)	0.864 (0.013)	24.266	98.478
aorsf-net	0.098 (0.071)	0.849 (0.068)	152.112	0.342
cif-extension	0.076 (0.005)	0.865 (0.011)	94.286	30.425
ranger-extratrees	0.075 (0.005)	0.848 (0.015)	7.014	6.801
nn-cox	0.072 (0.027)	0.828 (0.023)	15.582	14.415
aorsf-random	0.063 (0.006)	0.796 (0.015)	2.686	0.368
glmnet-cox	0.047 (0.044)	0.757 (0.153)	3.628	0.007
xgboost-cox	-0.011 (0.020)	0.871 (0.010)	6.431	0.009
xgboost-aft	-11.1 (1.34)	0.871 (0.012)	20.098	0.009
MESA; stroke, n = 6783, p = 48				
cif-rotate	0.024 (0.004)	0.760 (0.017)	273.629	37.321
obliqueRSF-net	0.024 (0.004)	0.763 (0.015)	355.997	289.216
cif-standard	0.024 (0.004)	0.758 (0.016)	23.726	98.376
aorsf-fast	0.024 (0.006)	0.761 (0.015)	1.099	0.313
aorsf-cph	0.023 (0.005)	0.755 (0.016)	4.501	0.322
ranger-extratrees	0.021 (0.003)	0.756 (0.015)	7.037	6.789
cif-extension	0.021 (0.002)	0.766 (0.017)	95.086	29.190
glmnet-cox	0.021 (0.010)	0.763 (0.017)	3.726	0.007
rsf-standard	0.018 (0.009)	0.742 (0.018)	3.127	1.058
aorsf-net	0.017 (0.027)	0.746 (0.045)	138.918	0.330
nn-cox	0.013 (0.009)	0.721 (0.050)	17.998	20.421
aorsf-random	0.013 (0.003)	0.710 (0.023)	2.582	0.338
xgboost-cox	0.000 (0.024)	0.760 (0.019)	4.044	0.008
xgboost-aft	-13.7 (1.50)	0.762 (0.016)	18.133	0.010
Monoclonal gammopathy; death, n = 1384, p = 8				
cif-rotate	0.157 (0.018)	0.743 (0.014)	15.346	4.755
aorsf-cph	0.155 (0.015)	0.741 (0.010)	1.157	0.087
aorsf-fast	0.154 (0.015)	0.741 (0.009)	0.393	0.087
obliqueRSF-net	0.153 (0.012)	0.742 (0.010)	229.434	12.810
aorsf-net	0.153 (0.014)	0.739 (0.009)	88.786	0.087
cif-standard	0.149 (0.013)	0.737 (0.010)	0.998	5.743
rsf-standard	0.147 (0.016)	0.735 (0.010)	2.002	0.201
aorsf-random	0.144 (0.013)	0.733 (0.011)	1.762	0.082
cif-extension	0.142 (0.009)	0.745 (0.012)	10.648	4.681
glmnet-cox	0.136 (0.020)	0.726 (0.014)	0.117	0.003

A.2: Index of prediction accuracy, time-dependent concordance statistic, and computational time required to fit and compute predictions for several learning algorithms across 31 risk prediction tasks. *(continued)*

	Scaled Brier	C-Statistic	Model fitting	Risk prediction
xgboost-cox	0.121 (0.011)	0.732 (0.011)	3.801	0.003
ranger-extratrees	0.115 (0.004)	0.742 (0.011)	0.058	0.198
nn-cox	0.031 (0.044)	0.612 (0.102)	15.825	0.684
xgboost-aft	-0.868 (0.152)	0.732 (0.012)	12.704	0.006
Monoclonal gammopathy; malignancy, n = 1384, p = 8				
glmnet-cox	0.016 (0.012)	0.654 (0.050)	0.104	0.002
aorsf-cph	0.011 (0.012)	0.644 (0.034)	0.592	0.041
aorsf-fast	0.010 (0.013)	0.641 (0.034)	0.193	0.042
ranger-extratrees	0.008 (0.007)	0.641 (0.033)	0.050	0.177
cif-extension	0.008 (0.009)	0.626 (0.026)	8.936	4.415
aorsf-random	0.007 (0.013)	0.633 (0.034)	0.519	0.041
aorsf-net	0.007 (0.013)	0.641 (0.032)	22.912	0.042
cif-standard	0.006 (0.009)	0.627 (0.029)	1.072	6.223
xgboost-cox	0.005 (0.017)	0.641 (0.036)	1.798	0.003
obliqueRSF-net	0.002 (0.023)	0.623 (0.040)	42.157	16.489
nn-cox	-0.004 (0.006)	0.502 (0.052)	10.457	0.704
rsf-standard	-0.010 (0.016)	0.615 (0.030)	0.733	0.075
cif-rotate	-0.025 (0.023)	0.550 (0.032)	12.854	4.638
xgboost-aft	-5.63 (1.08)	0.628 (0.039)	11.106	0.006
Movies released in 2015-2018; gross 1M USD, n = 551, p = 46				
cif-rotate	0.637 (0.023)	0.943 (0.007)	19.478	3.481
glmnet-cox	0.619 (0.032)	0.940 (0.009)	0.177	0.002
aorsf-net	0.531 (0.030)	0.929 (0.011)	52.072	0.044
aorsf-cph	0.523 (0.024)	0.926 (0.011)	0.785	0.042
rsf-standard	0.520 (0.022)	0.923 (0.011)	1.168	0.103
nn-cox	0.518 (0.065)	0.901 (0.027)	17.218	0.694
aorsf-fast	0.517 (0.028)	0.923 (0.013)	0.216	0.043
xgboost-cox	0.515 (0.028)	0.932 (0.009)	13.556	0.004
cif-standard	0.473 (0.026)	0.902 (0.018)	0.376	1.207
cif-extension	0.455 (0.025)	0.920 (0.013)	8.982	3.967
ranger-extratrees	0.432 (0.023)	0.900 (0.019)	0.047	0.108
obliqueRSF-net	0.319 (0.023)	0.909 (0.019)	154.491	9.054
aorsf-random	0.300 (0.035)	0.850 (0.030)	0.889	0.039
xgboost-aft	-0.474 (0.073)	0.928 (0.010)	34.905	0.007

A.2: Index of prediction accuracy, time-dependent concordance statistic, and computational time required to fit and compute predictions for several learning algorithms across 31 risk prediction tasks. *(continued)*

	Scaled Brier	C-Statistic	Model fitting	Risk prediction
Non-alcohol fatty liver disease; death, n = 17549, p = 24				
aorsf-cph	0.213 (0.008)	0.869 (0.005)	17.980	1.260
aorsf-fast	0.213 (0.009)	0.870 (0.005)	4.871	1.369
aorsf-net	0.211 (0.008)	0.865 (0.006)	452.725	1.292
obliqueRSF-net	0.210 (0.008)	0.869 (0.006)	1432.168	1054.002
rsf-standard	0.207 (0.009)	0.860 (0.005)	9.926	1.180
glmnet-cox	0.207 (0.010)	0.861 (0.005)	1.748	0.012
cif-standard	0.206 (0.007)	0.864 (0.006)	67.734	629.975
cif-rotate	0.191 (0.007)	0.865 (0.005)	263.866	61.085
ranger-extratrees	0.181 (0.007)	0.861 (0.005)	37.518	97.910
cif-extension	0.167 (0.003)	0.867 (0.006)	125.152	53.729
aorsf-random	0.141 (0.007)	0.839 (0.007)	9.722	1.365
xgboost-cox	0.020 (0.015)	0.877 (0.005)	9.143	0.018
nn-cox	0.000 (0.000)	0.558 (0.096)	22.004	120.407
xgboost-aft	-7.55 (0.727)	0.875 (0.005)	29.714	0.014
Primary biliary cholangitis; death, n = 276, p = 19				
aorsf-fast	0.425 (0.029)	0.905 (0.021)	0.069	0.018
aorsf-cph	0.414 (0.031)	0.902 (0.021)	0.150	0.018
cif-rotate	0.398 (0.037)	0.895 (0.021)	9.844	2.240
rsf-standard	0.388 (0.032)	0.891 (0.022)	0.093	0.038
aorsf-net	0.388 (0.077)	0.895 (0.030)	14.684	0.019
obliqueRSF-net	0.363 (0.029)	0.902 (0.022)	110.615	1.817
aorsf-random	0.350 (0.024)	0.891 (0.019)	0.283	0.019
cif-standard	0.345 (0.031)	0.899 (0.024)	0.186	0.363
cif-extension	0.342 (0.031)	0.897 (0.023)	5.197	2.313
glmnet-cox	0.335 (0.045)	0.881 (0.028)	0.115	0.002
ranger-extratrees	0.271 (0.025)	0.889 (0.026)	0.028	0.038
xgboost-cox	0.238 (0.105)	0.874 (0.024)	4.873	0.003
nn-cox	-0.019 (0.018)	0.548 (0.131)	10.566	0.240
xgboost-aft	-0.946 (0.320)	0.879 (0.021)	9.855	0.006
Rotterdam tumor bank; death, n = 2982, p = 11				
aorsf-net	0.165 (0.012)	0.761 (0.009)	156.800	0.190
obliqueRSF-net	0.163 (0.010)	0.760 (0.009)	452.125	37.754
aorsf-cph	0.162 (0.012)	0.758 (0.010)	2.537	0.198
aorsf-fast	0.160 (0.013)	0.756 (0.009)	0.796	0.198

A.2: Index of prediction accuracy, time-dependent concordance statistic, and computational time required to fit and compute predictions for several learning algorithms across 31 risk prediction tasks. *(continued)*

	Scaled Brier	C-Statistic	Model fitting	Risk prediction
cif-standard	0.159 (0.011)	0.759 (0.009)	4.692	22.441
rsf-standard	0.158 (0.013)	0.755 (0.008)	2.703	0.781
aorsf-random	0.153 (0.010)	0.752 (0.010)	2.959	0.184
cif-rotate	0.148 (0.012)	0.752 (0.012)	34.158	8.476
ranger-extratrees	0.139 (0.005)	0.749 (0.009)	2.888	2.552
xgboost-cox	0.132 (0.013)	0.754 (0.009)	3.742	0.004
cif-extension	0.130 (0.005)	0.751 (0.009)	22.061	8.711
glmnet-cox	0.118 (0.008)	0.731 (0.010)	0.219	0.004
nn-cox	-0.036 (0.096)	0.515 (0.044)	15.998	8.140
xgboost-aft	-1.37 (0.131)	0.761 (0.008)	14.219	0.007
Rotterdam tumor bank; recurrence, n = 2982, p = 11				
obliqueRSF-net	0.148 (0.011)	0.736 (0.010)	534.578	39.093
aorsf-net	0.146 (0.013)	0.735 (0.010)	162.899	0.193
cif-standard	0.144 (0.012)	0.734 (0.010)	4.570	22.729
aorsf-cph	0.144 (0.013)	0.734 (0.009)	2.769	0.211
aorsf-fast	0.142 (0.013)	0.733 (0.010)	0.869	0.210
aorsf-random	0.139 (0.011)	0.730 (0.009)	3.217	0.190
rsf-standard	0.138 (0.013)	0.730 (0.009)	2.838	0.633
ranger-extratrees	0.135 (0.008)	0.734 (0.010)	2.746	2.677
cif-rotate	0.130 (0.011)	0.726 (0.010)	36.702	8.773
cif-extension	0.119 (0.007)	0.731 (0.009)	22.630	8.891
glmnet-cox	0.117 (0.009)	0.727 (0.009)	0.224	0.004
xgboost-cox	0.114 (0.008)	0.730 (0.010)	3.367	0.004
nn-cox	-0.012 (0.031)	0.498 (0.056)	18.236	9.861
xgboost-aft	-1.05 (0.145)	0.734 (0.010)	14.853	0.007
Serum free light chain; death, n = 7874, p = 10				
aorsf-fast	0.250 (0.015)	0.826 (0.008)	2.023	0.596
aorsf-cph	0.250 (0.014)	0.825 (0.008)	6.558	0.594
glmnet-cox	0.247 (0.012)	0.820 (0.007)	0.492	0.006
obliqueRSF-net	0.247 (0.012)	0.821 (0.008)	1099.217	148.193
aorsf-net	0.245 (0.025)	0.821 (0.014)	294.157	0.564
ranger-extratrees	0.243 (0.010)	0.821 (0.008)	9.813	11.248
cif-standard	0.243 (0.012)	0.818 (0.009)	19.411	119.735
rsf-standard	0.242 (0.014)	0.816 (0.009)	4.514	0.563
aorsf-random	0.232 (0.012)	0.817 (0.009)	6.739	0.572

A.2: Index of prediction accuracy, time-dependent concordance statistic, and computational time required to fit and compute predictions for several learning algorithms across 31 risk prediction tasks. *(continued)*

	Scaled Brier	C-Statistic	Model fitting	Risk prediction
cif-rotate	0.227 (0.009)	0.819 (0.007)	65.161	21.299
cif-extension	0.202 (0.005)	0.821 (0.008)	39.535	20.315
xgboost-cox	0.091 (0.041)	0.824 (0.008)	5.971	0.008
nn-cox	0.001 (0.007)	0.603 (0.111)	23.138	25.985
xgboost-aft	-2.81 (0.306)	0.823 (0.008)	18.228	0.009
SPRINT; CVD death, n = 9361, p = 174				
aorsf-net	0.070 (0.008)	0.795 (0.012)	349.169	0.675
glmnet-cox	0.070 (0.012)	0.794 (0.010)	13.482	0.011
aorsf-fast	0.069 (0.006)	0.796 (0.010)	2.411	0.605
aorsf-cph	0.069 (0.006)	0.795 (0.011)	9.085	0.617
obliqueRSF-net	0.067 (0.005)	0.797 (0.012)	1012.843	426.872
rsf-standard	0.064 (0.007)	0.786 (0.015)	4.506	0.894
cif-standard	0.061 (0.004)	0.796 (0.011)	51.748	183.859
cif-rotate	0.060 (0.005)	0.788 (0.011)	964.703	114.180
ranger-extratrees	0.054 (0.003)	0.791 (0.013)	7.401	8.262
nn-cox	0.036 (0.021)	0.765 (0.018)	21.029	28.604
cif-extension	0.034 (0.002)	0.788 (0.011)	123.576	32.717
aorsf-random	0.026 (0.003)	0.746 (0.017)	5.646	0.745
xgboost-cox	0.007 (0.017)	0.797 (0.011)	7.242	0.014
xgboost-aft	-11.0 (0.929)	0.794 (0.012)	20.941	0.013
SPRINT; death, n = 9361, p = 174				
glmnet-cox	0.122 (0.012)	0.770 (0.010)	5.077	0.011
aorsf-cph	0.117 (0.008)	0.770 (0.009)	13.329	1.489
aorsf-fast	0.116 (0.009)	0.770 (0.008)	3.671	1.525
aorsf-net	0.113 (0.009)	0.768 (0.009)	608.998	0.987
obliqueRSF-net	0.112 (0.007)	0.767 (0.009)	2613.893	241.525
rsf-standard	0.110 (0.007)	0.763 (0.009)	6.285	0.695
cif-standard	0.106 (0.007)	0.764 (0.009)	49.138	191.018
nn-cox	0.098 (0.010)	0.757 (0.010)	38.077	31.856
ranger-extratrees	0.096 (0.005)	0.756 (0.009)	9.668	9.128
cif-rotate	0.091 (0.006)	0.745 (0.009)	1091.007	115.077
cif-extension	0.055 (0.002)	0.747 (0.010)	136.050	33.685
aorsf-random	0.052 (0.003)	0.719 (0.010)	9.318	1.016
xgboost-cox	0.028 (0.024)	0.772 (0.008)	9.389	0.013
xgboost-aft	-4.51 (0.336)	0.771 (0.008)	26.478	0.014

A.2: Index of prediction accuracy, time-dependent concordance statistic, and computational time required to fit and compute predictions for several learning algorithms across 31 risk prediction tasks. *(continued)*

	Scaled Brier	C-Statistic	Model fitting	Risk prediction
Systolic Heart Failure; death, n = 2231, p = 41				
obliqueRSF-net	0.114 (0.012)	0.747 (0.011)	376.279	24.724
cif-rotate	0.113 (0.013)	0.741 (0.010)	70.063	10.454
glmnet-cox	0.113 (0.013)	0.746 (0.011)	0.260	0.003
aorsf-net	0.112 (0.014)	0.744 (0.011)	119.643	0.160
aorsf-cph	0.111 (0.014)	0.745 (0.010)	1.972	0.153
cif-standard	0.110 (0.011)	0.744 (0.011)	3.959	15.682
aorsf-fast	0.110 (0.016)	0.745 (0.010)	0.625	0.153
rsf-standard	0.105 (0.012)	0.736 (0.009)	2.032	0.276
cif-extension	0.094 (0.006)	0.745 (0.011)	28.859	9.510
ranger-extratrees	0.092 (0.008)	0.738 (0.012)	2.893	1.729
xgboost-cox	0.091 (0.009)	0.745 (0.009)	4.478	0.004
aorsf-random	0.081 (0.005)	0.732 (0.012)	2.335	0.150
nn-cox	0.080 (0.024)	0.710 (0.032)	19.019	4.359
xgboost-aft	-2.04 (0.178)	0.742 (0.008)	13.559	0.007
VA lung cancer trial; death, n = 137, p = 8				
aorsf-net	0.204 (0.044)	0.796 (0.036)	9.921	0.012
aorsf-fast	0.204 (0.044)	0.794 (0.034)	0.047	0.011
aorsf-cph	0.202 (0.046)	0.793 (0.036)	0.097	0.013
cif-rotate	0.202 (0.059)	0.787 (0.038)	4.285	1.059
rsf-standard	0.179 (0.044)	0.787 (0.040)	0.067	0.025
cif-extension	0.176 (0.044)	0.794 (0.034)	3.541	1.194
glmnet-cox	0.160 (0.030)	0.787 (0.039)	0.078	0.002
aorsf-random	0.156 (0.043)	0.779 (0.039)	0.209	0.011
cif-standard	0.131 (0.035)	0.770 (0.036)	0.099	0.119
obliqueRSF-net	0.128 (0.031)	0.795 (0.029)	59.944	0.660
ranger-extratrees	0.092 (0.033)	0.778 (0.037)	0.021	0.027
xgboost-cox	0.062 (0.077)	0.747 (0.050)	1.139	0.002
xgboost-aft	-0.012 (0.141)	0.753 (0.046)	5.540	0.005
nn-cox	-0.028 (0.036)	0.525 (0.084)	11.338	0.123

A.3: Discrimination of relevant versus irrelevant variables for several techniques to estimate variable importance

| Max correlation | No. observations | accelerated oblique RSF | | | xgboost | | RSF |
		Negation	ANOVA	Permutation	SHAP	Gain	Permutation
Overall	Overall	76.1	73.9	73.3	69.5	64.5	67.8
Interactions							
Overall	Overall	58.0	57.4	58.0	54.3	48.8	57.1
30	500	55.4	54.7	56.0	48.0	42.3	55.3
30	1,000	56.6	56.0	57.9	53.2	48.5	55.4
30	2,500	61.4	59.0	63.6	61.8	60.7	60.2
15	500	53.3	53.5	53.0	45.1	39.1	55.0
15	1,000	57.5	55.2	56.9	51.2	44.6	54.5
15	2,500	62.2	58.9	62.5	61.3	59.6	61.7
0	500	50.6	52.7	52.5	43.2	40.3	53.6
0	1,000	57.8	58.5	55.1	53.9	43.0	55.2
0	2,500	67.2	68.4	64.5	70.6	61.5	62.5
Non-linear effects							
Overall	Overall	72.1	69.6	67.9	66.0	60.0	62.1
30	500	59.4	58.8	57.8	52.8	48.1	55.0
30	1,000	62.4	61.3	60.1	58.0	52.5	56.0
30	2,500	61.6	59.6	61.0	60.1	56.2	57.7
15	500	63.9	61.9	61.1	53.2	47.3	58.6
15	1,000	69.7	65.8	66.0	63.5	55.9	59.4
15	2,500	70.9	67.0	67.8	67.1	62.7	63.7
0	500	74.1	71.4	68.0	58.7	56.6	61.8
0	1,000	88.8	84.5	78.5	82.9	69.7	67.5
0	2,500	98.4	96.5	91.3	97.7	91.3	78.9
Combination effects							
Overall	Overall	78.5	75.8	75.0	70.6	65.1	68.2

A.3: Discrimination of relevant versus irrelevant variables for several techniques to estimate variable importance *(continued)*

Max correlation	No. observations	Negation	ANOVA	Permutation	SHAP	Gain	Permutation
30	500	65.3	63.3	63.7	55.7	50.1	59.5
30	1,000	67.8	65.7	65.4	61.7	55.8	60.8
30	2,500	69.4	66.8	68.3	65.4	62.0	64.3
15	500	71.1	68.3	66.8	58.3	51.8	62.3
15	1,000	75.6	71.3	71.9	66.6	59.6	64.4
15	2,500	79.1	74.7	76.8	73.3	69.2	70.1
0	500	83.2	80.7	76.1	65.1	61.5	67.2
0	1,000	95.8	92.5	88.5	89.8	78.6	76.3
0	2,500	99.8	99.4	97.8	99.7	97.8	88.9
Main effects							
Overall	Overall	90.9	88.8	88.5	84.7	82.4	82.9
30	500	79.3	77.1	75.1	70.1	66.2	71.0
30	1,000	83.9	80.7	80.0	76.9	73.7	74.4
30	2,500	87.0	83.7	85.2	82.2	80.8	79.1
15	500	85.9	83.0	82.1	74.2	70.2	74.8
15	1,000	91.0	87.6	88.2	84.5	80.5	80.2
15	2,500	94.3	91.6	93.5	89.8	88.5	86.7
0	500	97.2	95.5	93.2	85.5	84.3	85.1
0	1,000	99.9	99.8	99.4	99.4	97.5	94.6
0	2,500	100.0	100.0	100.0	100.0	100.0	99.8

References

Alessio Benavoli, Giorgio Corani, Janez Demšar, and Marco Zaffalon. Time for a change: a tutorial for comparing multiple classifiers through bayesian analysis. *The Journal of Machine Learning Research*, 18(1):2653–2688, 2017.

Paul Blanche, Jean-François Dartigues, and Hélène Jacqmin-Gadda. Estimating and comparing time-dependent areas under receiver operating characteristic curves for censored event times with competing risks. *Statistics in medicine*, 32(30):5381–5397, 2013.

Leo Breiman. Random forests. *Machine Learning*, 45(1):5–32, 2001.

Leo Breiman, Jerome H Friedman, Richard A Olshen, and Charles J Stone. *Classification and regression trees*. Routledge, 2017.

Yifan Cui, Ruoqing Zhu, Mai Zhou, and Michael Kosorok. Consistency of survival tree and forest models: splitting bias and correction. *arXiv preprint arXiv:1707.09631*, 2017.

Ben Goodrich, Jonah Gabry, Imad Ali, and Sam Brilleman. rstanarm: Bayesian applied regression modeling via Stan., 2022. URL `https://mc-stan.org/rstanarm/`. R package version 2.21.3.

Erika Graf, Claudia Schmoor, Willi Sauerbrei, and Martin Schumacher. Assessment and comparison of prognostic classification schemes for survival data. *Statistics in Medicine*, 18(17-18):2529–2545, 1999. URL `https://doi.org/10.1002/(SICI) 1097-0258(19990915/30)18:17/18%3C2529::AID-SIM274%3E3.0.CO;2-5`.

Frank E. Harrell, Robert M. Califf, David B. Pryor, Kerry L. Lee, and Robert A. Rosati. Evaluating the Yield of Medical Tests. *JAMA*, 247(18):2543–2546, 05 1982. ISSN 0098-7484. doi: 10.1001/jama.1982.03320430047030. URL `https://doi.org/10.1001/jama. 1982.03320430047030`.

David Heath, Simon Kasif, and Steven Salzberg. Induction of oblique decision trees. In *IJCAI*, volume 1993, pages 1002–1007. Citeseer, 1993.

Torsten Hothorn, Berthold Lausen, Axel Benner, and Martin Radespiel-Tröger. Bagging survival trees. *Statistics in medicine*, 23(1):77–91, 2004.

Torsten Hothorn, Kurt Hornik, and Achim Zeileis. Unbiased recursive partitioning: A conditional inference framework. *Journal of Computational and Graphical statistics*, 15 (3):651–674, 2006.

Hemant Ishwaran and Udaya B Kogalur. Consistency of random survival forests. *Statistics & probability letters*, 80(13-14):1056–1064, 2010.

Hemant Ishwaran and Min Lu. Standard errors and confidence intervals for variable importance in random forest regression, classification, and survival. *Statistics in medicine*, 38(4):558–582, 2019.

Hemant Ishwaran, Udaya B Kogalur, Eugene H Blackstone, and Michael S Lauer. Random survival forests. *The Annals of Applied Statistics*, pages 841–860, 2008.

Byron C Jaeger, D Leann Long, Dustin M Long, Mario Sims, Jeff M Szychowski, Yuan-I Min, Leslie A Mcclure, George Howard, and Noah Simon. Oblique random survival forests. *The Annals of Applied Statistics*, 13(3):1847–1883, 2019.

Michael W Kattan and Thomas A Gerds. The index of prediction accuracy: an intuitive measure useful for evaluating risk prediction models. *Diagnostic and prognostic research*, 2(1):1–7, 2018.

Rakesh Katuwal, Ponnuthurai Nagaratnam Suganthan, and Le Zhang. Heterogeneous oblique random forest. *Pattern Recognition*, 99:107078, 2020.

Max Kuhn and Hadley Wickham. *Tidymodels: a collection of packages for modeling and machine learning using tidyverse principles.*, 2020. URL https://www.tidymodels.org.

Scott Lundberg and Su-In Lee. A unified approach to interpreting model predictions, 2017.

Scott M Lundberg, Gabriel G Erion, and Su-In Lee. Consistent individualized feature attribution for tree ensembles. *arXiv preprint arXiv:1802.03888*, 2018.

Bjoern H Menze, B Michael Kelm, Daniel N Splitthoff, Ullrich Koethe, and Fred A Hamprecht. On oblique random forests. In *Joint European Conference on Machine Learning and Knowledge Discovery in Databases*, pages 453–469. Springer, 2011.

Karel GM Moons, Andre Pascal Kengne, Diederick E Grobbee, Patrick Royston, Yvonne Vergouwe, Douglas G Altman, and Mark Woodward. Risk prediction models: II. external validation, model updating, and impact assessment. *Heart*, 98(9):691–698, 2012a.

Karel GM Moons, Andre Pascal Kengne, Mark Woodward, Patrick Royston, Yvonne Vergouwe, Douglas G Altman, and Diederick E Grobbee. Risk prediction models: I. development, internal validation, and assessing the incremental value of a new (bio) marker. *Heart*, 98(9):683–690, 2012b.

Sreerama K Murthy, Simon Kasif, and Steven Salzberg. A system for induction of oblique decision trees. *Journal of Artificial Intelligence Research*, 2:1–32, 1994.

Nitesh Poona, Adriaan Van Niekerk, and Riyad Ismail. Investigating the utility of oblique tree-based ensembles for the classification of hyperspectral data. *Sensors*, 16(11):1918, 2016.

Xueheng Qiu, Le Zhang, Ponnuthurai Nagaratnam Suganthan, and Gehan AJ Amaratunga. Oblique random forest ensemble via least square estimation for time series forecasting. *Information Sciences*, 420:249–262, 2017.

Tom Rainforth and Frank Wood. Canonical correlation forests. *arXiv preprint arXiv:1507.05444*, 2015.

Carolin Strobl, Anne-Laure Boulesteix, Achim Zeileis, and Torsten Hothorn. Bias in random forest variable importance measures: Illustrations, sources and a solution. *BMC bioinformatics*, 8(1):25, 2007.

Terry Therneau. Survival package source code documentation, April 2022. URL https://github.com/therneau/survival/blob/5440691d44abea537b08aeb60153a31654d66a9b/noweb. original-date: 2016-04-28.

Tyler M Tomita, James Browne, Cencheng Shen, Jaewon Chung, Jesse L Patsolic, Benjamin Falk, Carey E Priebe, Jason Yim, Randal Burns, Mauro Maggioni, et al. Sparse projection oblique randomer forests. *Journal of machine learning research*, 21(104), 2020.

Hong Wang and Gang Li. A selective review on random survival forests for high dimensional data. *Quantitative bio-science*, 36(2):85, 2017.

Hong Wang and Lifeng Zhou. Random survival forest with space extensions for censored data. *Artificial intelligence in medicine*, 79:52–61, 2017.

Le Zhang and Ponnuthurai N Suganthan. Oblique decision tree ensemble via multisurface proximal support vector machine. *IEEE transactions on cybernetics*, 45(10):2165–2176, 2014.

Lifeng Zhou, Hong Wang, and Qingsong Xu. Random rotation survival forest for high dimensional censored data. *SpringerPlus*, 5(1):1–10, 2016.

Ruoqing Zhu. *Tree-based Methods for Survival Analysis and High-dimensional Data*. PhD thesis, The University of North Carolina at Chapel Hill, 2013.

Ruoqing Zhu, Donglin Zeng, and Michael R Kosorok. Reinforcement learning trees. *Journal of the American Statistical Association*, 110(512):1770–1784, 2015.